RESEARCH ARTICLE

WILEY

A CRISPR interference screen reveals a role for cell wall teichoic acids in conjugation in *Bacillus subtilis*

M. Michael Harden | Mary E. Anderson | Alan D. Grossman

Department of Biology, Massachusetts Institute of Technology, Cambridge, Massachusetts, USA

Correspondence
Alan D. Grossman, Department of Biology, Building 68-530, Massachusetts Institute of Technology, Cambridge, MA 02139, USA.
Email: adg@mit.edu

Abstract

Conjugative elements are widespread in bacteria and include plasmids and integrative and conjugative elements (ICEs). They transfer from donor to recipient cells via an element-encoded type IV secretion system. These elements interact with and utilize host functions for their lifecycles. We sought to identify essential host genes involved in the lifecycle of the integrative and conjugative element ICE*Bs1* of *Bacillus subtilis*. We constructed a library of strains for inducible knockdown of essential *B. subtilis* genes using CRISPR interference. Each strain expressed one guide RNA in ICE*Bs1*. We induced partial interference of essential genes and identified those that caused an acute defect in acquisition of ICE*Bs1* by recipient cells. This screen revealed that reducing expression of genes needed for synthesis of cell wall teichoic acids caused a decrease in conjugation. Using three different ways to reduce their synthesis, we found that wall teichoic acids were necessary in both donors and recipients for efficient conjugative transfer of ICE*Bs1*. Further, we found that depletion of wall teichoic acids caused cells involved in ICE*Bs1* conjugation to die, most likely from damage to the cell envelope. Our results indicate that wall teichoic acids help protect against envelope stress caused by active conjugation machines.

KEYWORDS
horizontal gene transfer, ICE*Bs1*, integrative and conjugative elements, mobile genetic elements

1 | INTRODUCTION

Horizontal gene transfer is fundamental to bacterial evolution, allowing for the rapid spread of genes involved in processes as diverse as antibiotic resistance, resource utilization, and pathogenesis (Frost et al., 2005; Soucy et al., 2015; Wiedenbeck & Cohan, 2011). Horizontal gene transfer is often mediated by conjugative elements which encode machinery to transfer a copy of the element from a host to a recipient via direct cell-to-cell contact. Although most studies of conjugative elements have focused on plasmids, integrative and conjugative elements (ICEs) appear to be the most abundant type of conjugative element and have been identified in every bacterial clade (Guglielmini et al., 2011).

ICEs normally reside integrated in a host chromosome where they are passively replicated and inherited. While in this inactive state, most ICE genes are not expressed. ICEs can be activated either stochastically or in response to certain conditions (i.e., DNA damage to the host, resource limitation), at which point a site-specific recombinase excises the ICE from the host chromosome to form a circular plasmid (Bañuelos-Vazquez et al., 2017). For conjugative

DNA transfer, the ICE plasmid DNA is nicked and a single strand is transferred out of the donor and into a recipient cell through the element-encoded type IV secretion system. Once transferred, the ssDNA becomes double stranded and can integrate into the chromosome of the new host, forming a stable transconjugant (Delavat et al., 2017; Johnson & Grossman, 2015; Wozniak & Waldor, 2010).

ICE*Bs1* is a relatively small ICE (~20 kb) (Auchtung et al., 2016) found in most isolates of the gram-positive bacterium *Bacillus subtilis*. Virtually all of the ICE*Bs1* genes required for conjugative transfer have homologs or analogs in other conjugative elements (Bhatty et al., 2013; Leonetti et al., 2015). ICE*Bs1* is normally integrated into *trnS-leu2* (a tRNA gene). When integrated, only a few ICE*Bs1* genes are expressed. Gene expression and subsequent excision are induced during the RecA-dependent SOS response, or in the presence of other *B. subtilis* cells lacking a copy of the element (Auchtung et al., 2005; Bose et al., 2008). ICE*Bs1* can be experimentally activated, typically in 50-90% of cells in a population by overproducing the element-encoded regulatory protein RapI, enabling high frequencies of transfer that make it quite useful for studying conjugation (Auchtung et al., 2005; Lee et al., 2007).

The life cycles of all mobile genetic elements depend on various host functions. In this study, we sought to identify essential host genes that are necessary for the life cycle of ICE*Bs1*. We were most interested in identifying host functions that affect conjugation, rather than host functions that affect the production of the ICE proteins (e.g., transcription, translation) or the replication of ICE DNA (Lee et al., 2010).

We used CRISPR interference (CRISPRi) to block transcription of essential *B. subtilis* genes and identified host factors in an ICE*Bs1* donor that are important for transfer. Several genes were identified in this screen and we chose to focus on those involved in the synthesis of cell wall teichoic acids.

Wall teichoic acids (WTAs) are polyol-phosphate repeats that are attached to the peptidoglycan cell wall of gram-positive bacteria [reviewed in: (Brown et al., 2013; Swoboda et al., 2010)]. In *B. subtilis* 168, WTAs comprise 45-60 repeats of glycerol 3-phosphate (Pollack & Neuhaus, 1994). These repeats can be modified by WTA-tailoring enzymes, most notably by D-alanylation and glycosylation (Allison et al., 2011; Perego et al., 1995). In *B. subtilis* 168, WTAs are synthesized by enzymes encoded by the *tag* genes (*tagO*, *tagAB*, *tagDEF*, and *tagGH*). TagO catalyzes the first step of WTA biosynthesis (D'Elia et al., 2006). TagA catalyzes the second step and is the first committed step (D'Elia, Henderson et al., 2009). WTAs are not strictly required for cell growth. WTA-depleted *B. subtilis* cells are viable but slow-growing, and have significant alterations in cell shape and cell separation (D'Elia et al., 2006). Some WTA biosynthesis genes (*tagBDFGH*) are conditionally essential, likely because their deletion results in either the accumulation of toxic intermediates or the sequestration of vital cellular resources (D'Elia, Millar et al., 2006, 2009).

WTAs are a critical component of the bacterial cell wall and have diverse functions, although their specific roles are not well understood. WTAs regulate autolysins (cell wall-degrading enzymes) in multiple species of bacteria. In both *S. aureus* and *B. subtilis*, certain autolysins involved in cell division exhibit improper localization patterns in the absence of WTAs, and it is thought that the presence of WTAs may exclude those autolysins from portions of the cell wall (Frankel & Schneewind, 2012; Schlag et al., 2010; Yamamoto et al., 2008). Proper localization of *B. subtilis* LytE, an autolysin required for cell elongation, is also disrupted in WTA-depleted cells (Kasahara et al., 2016). WTA-lacking bacteria are also more prone to autolysis and more sensitive to the activity of peptidoglycan-lytic enzymes (Bera et al., 2007; Schlag et al., 2010; Wecke et al., 1997).

WTAs may also have a role in peptidoglycan biosynthesis. Mutants of *B. subtilis* exhibit cell-shape defects and have walls of irregular thickness (D'Elia et al., 2006), suggesting that WTAs may be important for organizing the peptidoglycan biosynthesis machinery (Brown et al., 2013). Depletion of WTAs can sensitize bacteria to β-lactams, which may suggest that the two processes are interconnected (Campbell et al., 2011; Farha et al., 2013). WTAs have been proposed to have several other functions, including in virulence (Weidenmaier & Peschel, 2008), bacteriophage attachment (Yasbin et al., 1976; Young, 1967), competence (Mirouze et al., 2018), and cell-cell and cell-surface adhesion (Gross et al., 2001; Walter et al., 2007).

In work described here, we found that wall teichoic acids are necessary in both ICE*Bs1* donor and recipient cells for efficient transfer of the element. The activity of the ICE*Bs1* conjugation machinery was toxic to cells that were depleted of wall teichoic acids, and these cells appeared to die from damage to the cell envelope caused by the conjugation machinery.

2 | RESULTS

2.1 | A CRISPRi screen for essential host genes involved in conjugation

2.1.1 | Rationale

We sought to identify host genes in an ICE*Bs1* donor that are important for transfer of the element. Previously, we used Tn-seq to identify genes in recipients that are involved in acquisition of ICE*Bs1* via conjugation (Johnson & Grossman, 2014). Several of the genes identified were also important in donors (Johnson & Grossman, 2014). In preliminary experiments, we screened individual insertion mutants from a transposon insertion library and were unable to reliably identify candidate genes in donors that affected conjugation. Therefore, we focused on a screen that would readily identify essential genes that have a role in conjugation.

2.1.2 | CRISPRi knockdown of essential genes

We used a *B. subtilis* CRISPRi system (Peters et al., 2016) to reduce expression of essential genes in *B. subtilis*, and screened for those

that caused a defect in conjugation. Briefly, the system comprises a catalytically dead Cas9 nuclease from *Streptococcus pyogenes* (dCas9) under the regulation of the xylose-inducible promoter Pxyl and a constitutively expressed single-guide RNAs (sgRNA) containing a 20 nt region corresponding to the target gene of interest. When dCas9 is produced via the addition of xylose, it complexes with the sgRNA and stably binds to the host gene specified by the targeting region of the sgRNA. This interaction sterically blocks transcript elongation, thereby lowering expression of the targeted gene or operon. The library of sgRNAs used in this study (a gift of Peters et al.) collectively targeted a set of 289 proposed essential *B. subtilis* genes (Peters et al., 2016), 257 of which were subsequently verified to be essential in a systematic gene knockout analysis (Koo et al., 2017).

2.1.3 | CRISPRi library in ICE*Bs1*

We created a library of donor strains in which ICE*Bs1* could be induced by overproducing its activator protein RapI. All donor strains contained a xylose-inducible Pxyl-*dcas9* integrated into the host chromosome. Each donor strain also had one constitutively expressed sgRNA allele (Pveg-*sgRNA*) integrated into a site in ICE*Bs1* that is not needed for transfer. In this way, we constructed a pooled library of donor strains with each individual donor strain representing a knockdown of one essential *B. subtilis* gene (Figure 1a).

2.1.4 | The screen

We used the CRISPRi system in ICE*Bs1* to partially decrease expression of essential genes. We used partial (0.01% xylose) rather than full expression of *dcas9* because we were concerned that high levels, in combination with an sgRNA targeting an essential gene, would cause a significant fitness defect of each donor strain and would have strongly biased or interfered with the screen. Expression of ICE*Bs1* was activated and the donor library was mixed with recipients and transconjugants were selected (Experimental Procedures). The overall mating efficiency of this pooled library (0.17%) was similar to that of a control strain with a knockdown targeted to a nonessential gene (MMH233, 0.36%), indicating that the partial knockdown treatment did not have a substantial global effect on conjugation.

We used next-generation sequencing to determine the relative abundance of sgRNA alleles in a sample of: (1) donors harvested immediately prior to mating and (2) the pool of transconjugants. Importantly, the target of a gene knockdown is specified by the sgRNA encoded within ICE*Bs1* itself. As a consequence, every transconjugant generated by this library contains a genetic record of the donor strain that produced it. We can determine the relative mating efficiency of a given donor strain by pooling the population of transconjugants, collectively sequencing their sgRNA alleles, and then determining which sgRNAs differ in abundance compared with the pre-mating donor population. If a knockdown compromised ICE*Bs1* mating efficiency, then the sgRNA corresponding to that

gene would be underrepresented in the resulting pool of transconjugants. Conversely, if a knockdown improved ICE*Bs1* mating efficiency, then the sgRNA allele corresponding to the that gene would be overrepresented in the pool of transconjugants.

Decreased expression of most of the essential genes had little or no effect on mating efficiency (Figure 1b). We compared the relative abundance of each sgRNA in the transconjugant population to the pre-mating donor population and found that >80% of knockdowns resulted in less than a four-fold change in the abundance of the sgRNA gene in the transconjugant pool relative to the starting population (Figure 1b, points above diagonal dotted line). We did not detect an increase greater than four-fold in any of the sgRNA genes in transconjugants, indicating that none of the essential genes seemed to be substantially inhibiting the function of ICE*Bs1*.

We chose to focus on those genes that caused less than or equal to four-fold effects to increase the chances that observed effects were robust and significant. We also focused on knockdown strains that were well represented in the donor pool (Figure 1b, points to the right of the horizontal line, >0.01%), and that had the largest decrease in conjugation. Of this subset of knockdowns, most were involved in processes that directly affect the production of the conjugation machinery, including genes involved in translation, protein secretion, and protein folding. We did not study these.

Knockdown of *tagA* resulted in the most severe transfer defect out of all genes tested in the screen. *tagA* is needed for biosynthesis of WTAs. Strains with knockdowns of other WTA biosynthesis genes (*tagO*, *tagB*, *tagD*, *tagF*, *tagG*, and *tagH*) were also present in the library, and two of these knockdowns (*tagD* and *tagF*) also resulted in greater than four-fold defects in conjugation (~10- and ~4.5-fold, respectively; Table S1). We decided to further investigate the role of *tagA* and WTA biosynthesis in conjugation.

We note that several other genes were also identified as candidates for affecting conjugation, including genes whose products are involved in peptidoglycan synthesis, cell shape, restriction-modification, and other cellular functions (Table S1). For example, reduced expression of *rny* (encoding the endoribonuclease RNase Y) and *mnt* (encoding a component of an ABC manganese transporter) appeared to cause an ~20-fold and ~1000-fold decrease in conjugation, respectively, in the context of the CRISPRi screen (Table S1). Although we have not validated these findings, some of these genes may have interesting roles in the life cycle of ICE*Bs1*.

2.2 | WTAs are necessary in an ICE*Bs1* donor for efficient transfer

To validate the apparent effect of *tagA* revealed in the CRISPRi screen, we directly tested for effects of *tagA* on ICE*Bs1* conjugation in several ways. First, we measured the conjugation efficiency {stable transconjugants per donor; each measured as colony-forming units (CFUs)} from a homogenous population of donor cells in which *tagA* expression was inhibited by CRISPRi. This is in contrast to the screen which used a population of strains representing the entire
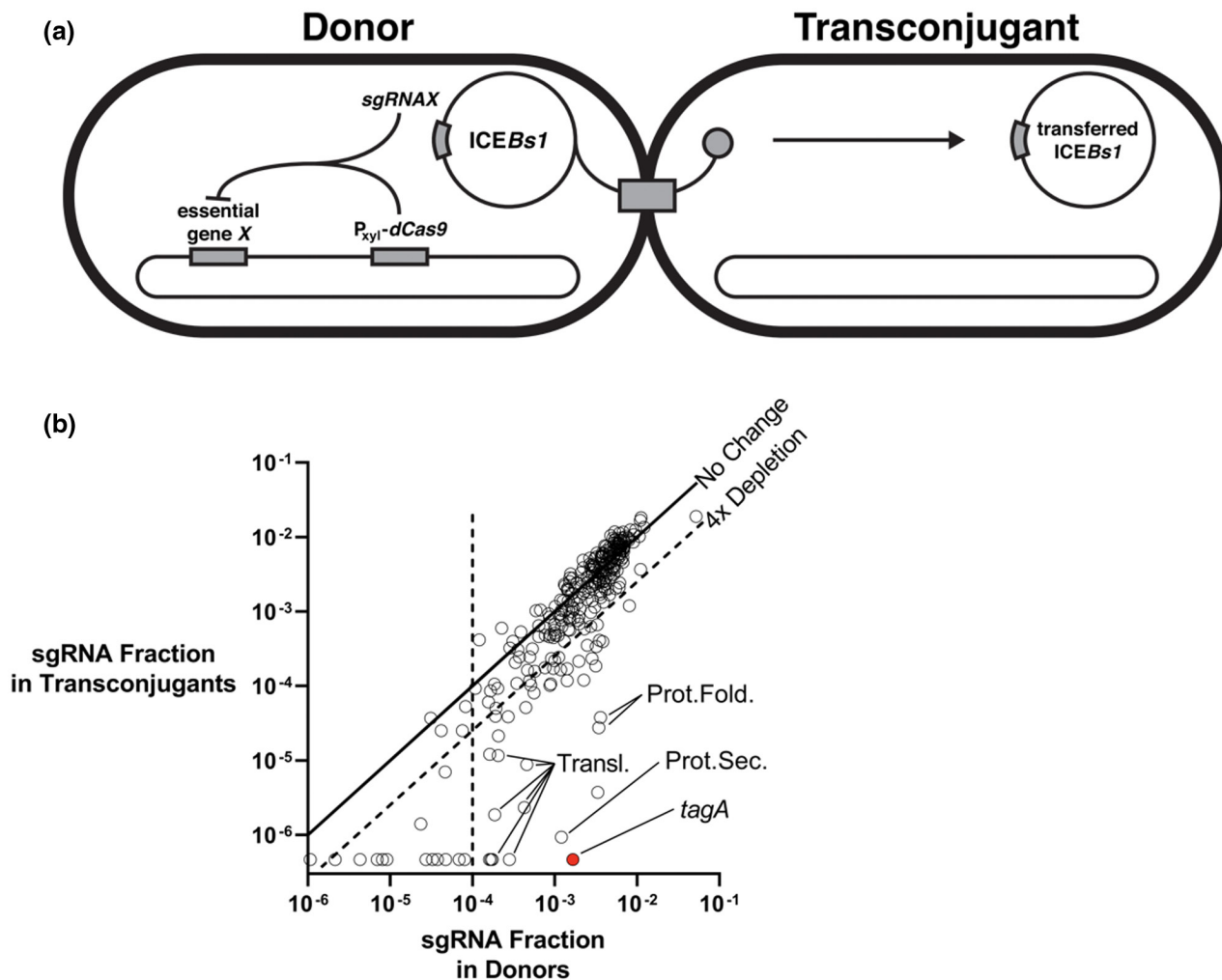
FIGURE 1 CRISPRi screen identifies essential host gene knockdowns that affect transfer of ICE*Bs1*. (a) Experimental design of CRISPRi screen. Each ICE*Bs1* donor contains a xylose-inducible Pxyl-*dcas9* allele integrated into a non-ICE locus of the host chromosome and a constitutively expressed sgRNA allele integrated into ICE*Bs1*. Each sgRNA allele has a unique 20 bp targeting region which specifies a knockdown of a single proposed essential gene. A pooled library of inducible ICE*Bs1* donor strains (*lacA*::{Pxyl-dcas9 (*ermR*)} Δ*amyE117*::{P*spank-rapI* (*spc*)} Δ*rapI-phrI*::(*amyE kan*)::{P*veg-sgRNA*^{X} (*cat*)}), collectively representing partial knockdowns of all *B. subtilis* essential genes, was induced to mate with an ICE*Bs1*^{0} recipient strain (CAL89). If a knockdown results in a transfer defect, the corresponding sgRNA would be less abundant in the transconjugant population relative to the pre-mating donor population. The transconjugant is shown prior to integration of ICE*Bs1* into the chromosome. (b) Results of CRISPRi screen. The pools of sgRNA alleles in the pre-mating donor population and post-mating transconjugant population were sequenced and compared. Each point corresponds to one sgRNA allele included in the screen. The x- and y-axes correspond to the fractions of the donor and transconjugant pools, respectively, that an sgRNA allele represents. The solid diagonal line ($x = y$) represents no change in abundance between the two populations. Points falling below the diagonal dashed line correspond to alleles that were > greater than fourfold depleted in the transconjugant pool. Points to the left of the vertical dashed line represent sgRNAs that were largely depleted from the donor pool prior to mating (<0.01%). Select sgRNAs are annotated by name or functional grouping. More detailed results are reported in Table S1

CRISPRi library. As anticipated, decreasing *tagA* expression in an ICE*Bs1* donor resulted in an acute drop in conjugation (Figure 2a). The severity of the defect increased as *tagA* expression decreased, with the strongest knockdown resulting in no detectable ICE*Bs1* transfer (<1 × 10^{-3}).

We inhibited WTA synthesis in ICE*Bs1* donors in two additional ways. In one, we made three different donor strains, each with one of three *tag* operons (*tagO*, *tagAB*, or *tagDEF*) under the control of the LacI-repressible isopropyl-ß-D-thiogalactopyranoside (IPTG)-inducible promoter Pspank. With low expression levels (little or no

IPTG), these strains exhibited cell shape defects characteristic of WTA depletion (Figure S1) (D'Elia et al., 2006; Mirouze et al., 2018). We grew these strains in different IPTG concentrations (ranging from 0 to 100 μM) for approximately six generations and then measured effects on conjugation. Reducing expression of any of the three operons (*tagO*, *tagAB*, *tagDEF*) resulted in an acute drop in conjugation (Figure 2b–d). In all three cases, mating efficiency dropped more than 1000-fold at the lowest level of expression tested (no IPTG). Whereas disruption of downstream WTA biosynthesis genes (*tagB*, *tagD*, *tagF*) can impact Lipid II production by sequestering the
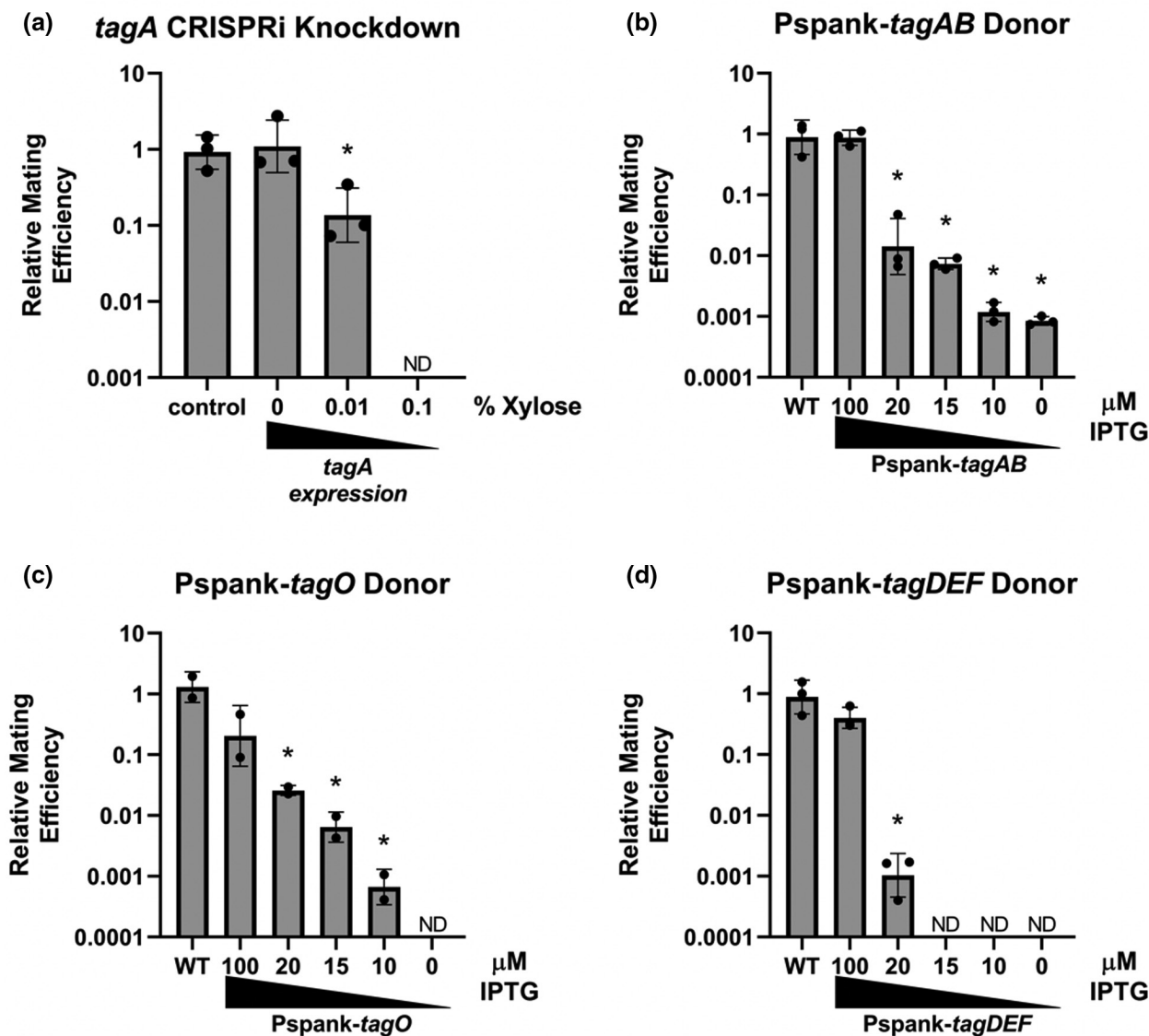
FIGURE 2 Decreased expression of *tag* genes causes a decrease in conjugation. Expression of *tag* genes was inhibited in ICE*Bs1* donors and the resulting impact on mating efficiency was examined. Relative mating efficiencies are reported as number of transconjugants per pre-mating donor normalized to the wild type control. Graphs show averages and standard deviations of log-transformed data from two or three biological replicates. * indicates average relative mating efficiency was significantly different from the wild type control (one-way ANOVA and Dunnett's multiple comparisons test). (a) An individual ICE*Bs1* donor strain with a xylose-inducible CRISPRi knockdown of *tagA* (MMH527) was induced to mate with an ICE*Bs1*^{0} recipient strain (CAL89). Knockdowns were induced via incubation with either 0, 0.01%, or 0.1% xylose. An ICE*Bs1* donor strain with a control knockdown was used as the control (MMH525, *cgeD*, 0.1% xylose). ND indicates mating efficiency was below limit of detection (<.001). Average mating efficiency of the control was 8.8×10^{-4} with a standard deviation of 4.1×10^{-4}. (b–d) ICE*Bs1* donor strains were constructed in which a WTA biosynthesis operon, either *tagAB* (b; MMH578), *tagO* (c; MMH577), or *tagDEF* (d; MMH608), was placed under the control of the IPTG-inducible promoter Pspank. Each donor was mated with an ICE*Bs1*^{0} recipient strain (CAL89). Expression of the *tag* operon was controlled by growing the donor strain at the indicated IPTG concentration. A wild type ICE*Bs1* donor (CAL874) was used as a control. ND indicates mating efficiency was below limit of detection (<0.0006 for c; <0.002, 0.002, and 0.001 for the 15 μM, 10 μM, and 0 μM treatments in D, respectively). Average mating efficiency and standard deviation of the controls were $7.8 \times 10^{-4} \pm 4.0 \times 10^{-4}$, $6.9 \times 10^{-4} \pm 6.2 \times 10^{-4}$, and $6.6 \times 10^{-4} \pm 3.7 \times 10^{-4}$ for b, c, and d respectively

cellular supply of undecaprenyl phosphate in the blocked WTA synthesis pathway, reducing *tagO* expression or inhibiting TagO (the first step of WTA biosynthesis) does not result in this sequestration (D'Elia, Millar, et al., 2009). Accordingly, these results demonstrate that the ICE*Bs1* transfer defect is not a consequence of Lipid II depletion.

We also inhibited WTA synthesis using a low concentration (1 μg/ml) of the antibiotic tunicamycin. At this concentration, tunicamycin specifically inhibits WTA biosynthesis in gram-positive bacteria by blocking the activity of TagO (Campbell et al., 2011; Pooley & Karamata, 2000). At higher concentrations (>10 μg/ml) it inhibits peptidoglycan biosynthesis and cell growth (Campbell et al., 2011;

Price & Tsvetanova, 2007). Importantly, inhibiting WTA biosynthesis with tunicamycin (1 µg/ml) for approximately three generations (60 min) in an ICE*Bs1* donor decreased ICE*Bs1* transfer ~150-fold (Figure 3a). Based on these results, we infer that WTAs are likely necessary for efficient transfer of ICE*Bs1*. Alternatively, it is formally possible that the biosynthetic activity of TagO and WTA biosynthesis per se is important and not accumulation of WTAs themselves.

We found that WTAs themselves are necessary for efficient ICE transfer, rather than WTA biosynthesis. We inhibited WTA biosynthesis without substantially depleting cells of WTAs by treating ICE*Bs1* donors with tunicamycin for 1 min prior to mating. Under these conditions, there would be no substantial decrease in the amount of WTAs, but biosynthesis should be inhibited. There was little or no defect in conjugation of ICE*Bs1* under these conditions
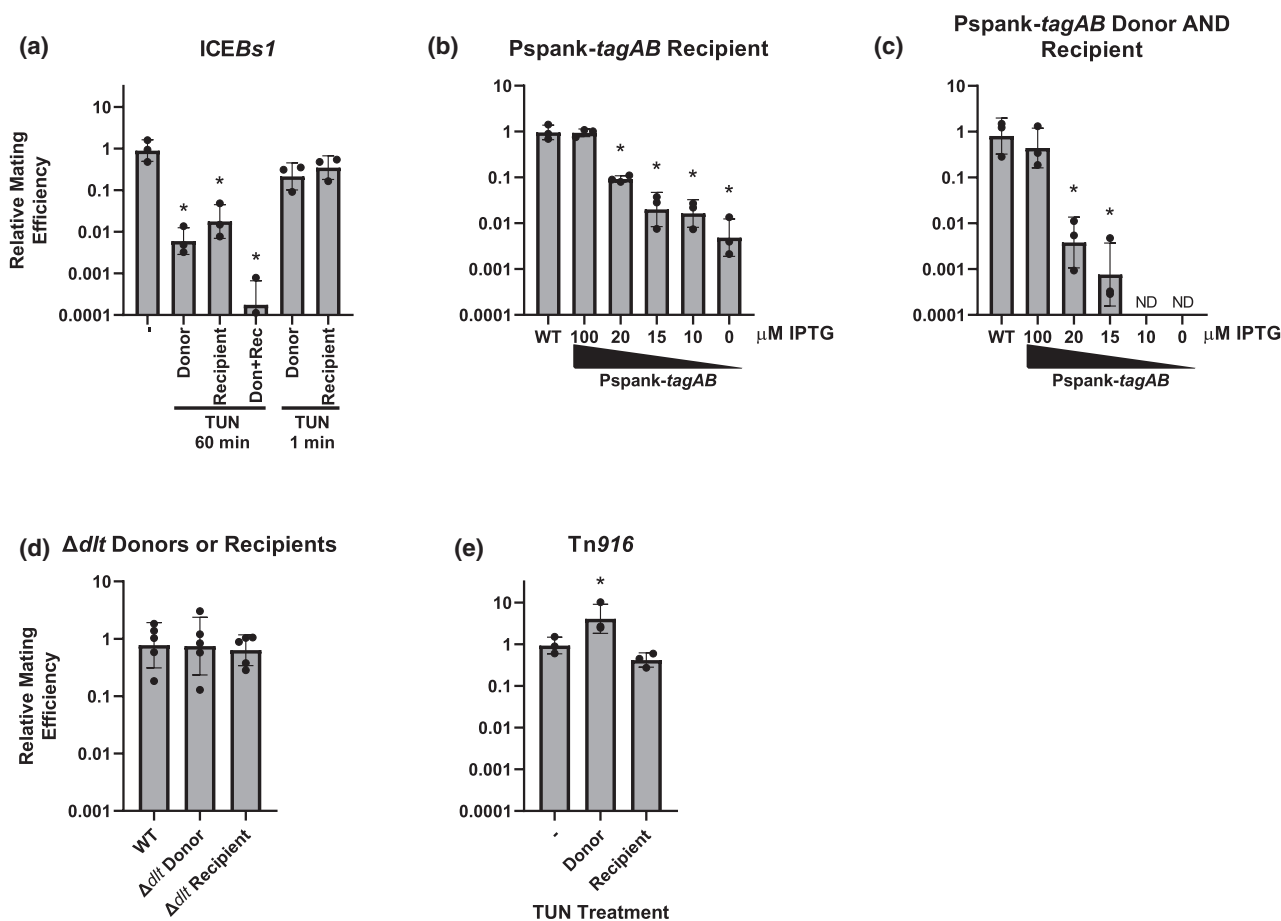
FIGURE 3 WTAs are necessary in both ICE*Bs1* donors and recipients for efficient transfer of the element. WTA biosynthesis or WTA D-alanine modification was inhibited or prevented in ICE donors and ICE^0 recipients, and the resulting impacts on mating efficiencies were examined. Relative mating efficiencies are reported as described in Figure 2. Graphs show averages and standard deviations of log-transformed data from three biological replicates. * indicates average relative mating efficiency was significantly different from the wild type or untreated control (one-way ANOVA and Dunnett's multiple comparisons test, $p < .05$). (a) WTA biosynthesis was inhibited in an ICE*Bs1* donor (MMH550), an ICE*Bs1*^{0} recipient (MMH676), or both by adding the TagO-inhibiting drug tunicamcyin (1 µg/ml). The drug was added either 60 min prior to mating to block synthesis and deplete WTAs, or 1 min prior to mating to block WTA synthesis without substantial WTA depletion. Average mating efficiency of the untreated control was 3.6×10^{-3} with a standard deviation of 2.3×10^{-3}. (b) An ICE*Bs1* donor (CAL874) was mated with an ICE*Bs1*^{0} recipient in which the WTA biosynthesis operon *tagAB* had been placed under the control of Pspank (MMH584). Expression of *tagAB* was controlled by growing the recipient strain at the indicated IPTG concentrations. A wild type recipient (CAL89) was used as a control. Average mating efficiency with the wild type control was 6.1×10^{-4} with a standard deviation of 2.3×10^{-4}. (c) The Pspank-*tagAB* donor strain from Figure 2b (MMH578) was mated with the Pspank-*tagAB* recipient strain from 3b (MMH584). Both strains were grown at the indicated IPTG concentration. ND indicates relative mating efficiency was below the limit of detection (<0.0007 and <0.0008 for the 10 µM and 0 µM treatments, respectively). Average mating efficiency of the wild type control was 1.3×10^{-3} with a standard deviation of 8.2×10^{-4}. (d) Donors (MMH541) or recipients (MMH545) that were defective in D-alanylation of WTAs (*ΔdltABCDE::cat*) were used in conjugation experiments. *ΔdltABCDE* donors (MMH541) were mated with a wild type recipient (CAL85). *ΔdltABCDE* recipients (MMH545) were mated with a wild type donors (CAL874). The wild type donor (CAL874) was mated with the wild type recipient (CAL85) as a control. Average mating efficiency with the control was 2.4×10^{-3} with a standard deviation of 1.6×10^{-3}. (e) The effect of inhibiting WTA biosynthesis on a Tn*916* donor (CMJ253) or recipient (MMH676) was tested by adding tunicamycin to growing cells 60 min prior to mating. Average mating efficiency of the untreated control was 4.5×10^{-6} with a standard deviation of 2.1×10^{-6}

(Figure 3a). Together, our results demonstrate that WTAs are required in donor cells for efficient transfer of ICE*Bs1*.

2.3 | WTAs are necessary in an ICE*Bs1* recipient for efficient transfer

We wished to determine if WTAs are also needed in recipients for efficient acquisition of ICE*Bs1*. We treated recipients with tunicamycin for 1 h and found that acquisition of ICE*Bs1* was reduced ~50-fold (Figure 3a). As with donors, blocking WTA biosynthesis in the recipient with tunicamycin treatment for only 1 min prior to mating caused little or no defect in acquisition of ICE*Bs1* (Figure 3a), indicating that WTAs themselves (and not simply WTA biosynthesis) are necessary in the recipient for efficient mating.

We also reduced WTAs in recipients by decreasing expression of *tagAB* (from a P*spank-tagAB* fusion) by growing cells in low concentrations (or in the absence) of IPTG for approximately six generations. With the lowest level of expression (no IPTG), the mating efficiency into the WTA-depleted recipients was decreased ~200-fold relative to that of cells grown in 100 μM IPTG or wild type cells (Figure 3b).

Reducing WTAs in both donors and recipients caused a defect in mating that was more severe than reduction in either donor or recipient alone (Figure 3a,c). This was true following treatment of donors and recipients with tunicamycin (Figure 3a) or growing both donors and recipients containing P*spank-tagAB* in low concentrations of IPTG (Figure 3c).

Based on these results, we conclude that WTAs in both donors and recipients are important for efficient conjugation of ICE*Bs1*. WTAs could be needed for the proper function, assembly, or regulation of the conjugation machinery, for establishing or maintaining cell-cell contact to enable mating, or for cell viability during mating.

2.4 | D-alanylation of wall teichoic acids is not needed for efficient transfer of ICE*Bs1*

In *B. subtilis*, WTA polymers may be tailored by the addition of D-alanine moieties. The degree of WTA D-alanylation varies under different cellular conditions, and the cationic D-alanine moieties are thought to affect the function of WTAs by lessening the extent of the polymer's negative charge (Neuhaus & Baddiley, 2003). WTA D-alanylation occurs outside the cell and is mediated by the proteins encoded by the *dltABCDE* operon (Perego et al., 1995). We constructed ICE*Bs1* donor and recipient strains that lacked the *dltABCDE* operon to determine whether D-alanine-modified WTAs are needed for efficient transfer of ICE*Bs1*.

We found that D-alanylation of WTAs is not necessary for efficient transfer or acquisition of ICE*Bs1*. The mating efficiency of ICE*Bs1* was not significantly affected by the use of either a Δ*dltABCDE* ICE*Bs1* donor or recipient (Figure 3d). Based on these results, we conclude that the presence of D-alanine moieties on either ICE*Bs1* donor or recipient WTAs is not necessary for efficient transfer of the element.

2.5 | WTAs are not necessary for transfer of the broad host range ICE Tn*916*

We tested for effects of WTAs on conjugative transfer of Tn*916*, a small (~18 kb) ICE that confers tetracycline resistance to its host. Activity of Tn*916* is increased several fold in the presence of tetracycline (Showsh & Andrews, 1992). Whereas the natural host of ICE*Bs1* appears to be limited to *B. subtilis*, Tn*916* is found in a broader range of gram-positive bacteria (Roberts & Mullany, 2009) and, although not its natural host, works quite well in *B. subtilis* (Celli & Trieu-Cuot, 1998; Christie et al., 1987; Johnson & Grossman, 2014).

FIGURE 4 WTA-depleted ICE*Bs1* donors and recipients do not efficiently mate because they experience lethal cell envelope damage. (a) The use of an osmoprotective mating surface eliminates the WTA-depletion ICE*Bs1* transfer defect. WTAs were depleted by treating ICE*Bs1* donors (MMH862) or recipients (MMH797) with 1 μg/ml tunicamycin for 60 min as in Figure 3a, and strains were mated on either a standard mating surface (1× Spizizen's salts agar) or on an osmoprotective mating surface (1× MSM agar). Graph shows averages and standard deviations of log-transformed data from three biological replicates. * indicates average relative mating efficiency was significantly different from 1 (one-way ANOVA and Dunnett's multiple comparisons test, $p < 0.05$). Average mating efficiency of the wild type under non-protective conditions was 4.3×10^{-3} with a standard deviation of 2.1×10^{-3}. (b) WTA biosynthesis was inhibited by treating ICE*Bs1* donors (MMH862) or recipients (MMH797) with 1 μg/ml tunicamycin as in 4a. Strains were mated on either a standard mating surface (1× Spizizen's salts agar) or on a 1× MSM agar surface lacking sucrose. Graph shows averages and standard deviations of log-transformed data from three biological replicates. * indicates average relative mating efficiency was significantly different from 1 (Student's one-way ANOVA and Dunnett's multiple comparisons test, $p < 0.05$). Average mating efficiency for the untreated control (on SPIZ) was 1.3×10^{-3} with a standard deviation of 1.5×10^{-3}. (c) WTA-depleted ICE*Bs1* donors do not exhibit an observable drop in viability at the population level during mating. An ICE*Bs1* donor strain (MMH862) was treated or not treated with tunicamycin and induced to mate with an ICE[0] recipient (MMH797) as in 4a and 4b, and the number of viable post-mating donors was compared with the number of pre-mating donors. Each dot represents data from a single independent experiment ($n = 6$). The central bars represent the average. (d) WTA-depleted cells engaging in ICE*Bs1* mating are more likely to sustain lethal membrane damage. ICE*Bs1* Δ*yddJ* cells with (MMH794) or without (MMH788) an IPTG-inducible ICE allele were cultured with IPTG and ± tunicamycin, concentrated on an agar pad containing propidium iodide, and tracked for 2 h via fluorescence microscopy. The percentage of PI-stained cells was recorded. Data are the averages of three biological replicates. Error bars indicate standard deviation. * indicates the averages of the two treatments are significantly different (one-way ANOVA and Tukey's multiple comparisons test, $p < .05$)

We found that unlike ICEBs1, Tn916 transfer was not significantly affected when WTA biosynthesis was inhibited. We depleted WTAs in Tn916 donors or recipients with tunicamycin (1 µg/ml) for 60 min. The mating efficiency following treatment of recipients was similar to that of untreated recipients, and that of donors appeared to increase slightly (Figure 3e). This indicates that the decrease in transfer of ICEBs1 in response to WTA depletion is probably not due to a general effect on host physiology, or an inability of cells to contact each other, unless the presence of Tn916 compensates for these alterations. This differential effect of WTAs on ICEBs1 compared with Tn916 highlights a difference between conjugation mediated by these elements.

2.6 | An osmoprotective mating surface bypasses the need for WTAs in ICEBs1 conjugation

Cell wall hydrolases encoded by conjugative elements are essential for conjugation in gram-positive bacteria (Arends et al., 2013; Bantwal et al., 2012; DeWitt & Grossman, 2014; Laverde Gomez et al., 2014). As mentioned above (Introduction), WTAs are important regulators of the activity of host-encoded cell wall hydrolases (autolysins) and are necessary for the proper localization of autolysins in several species (Bonnet et al., 2018; Frankel & Schneewind, 2012; Schlag et al., 2010; Yamamoto et al., 2008). Bacteria depleted of WTAs are more prone to autolysis and are more sensitive to

(a)

(b)

(c)

(d)
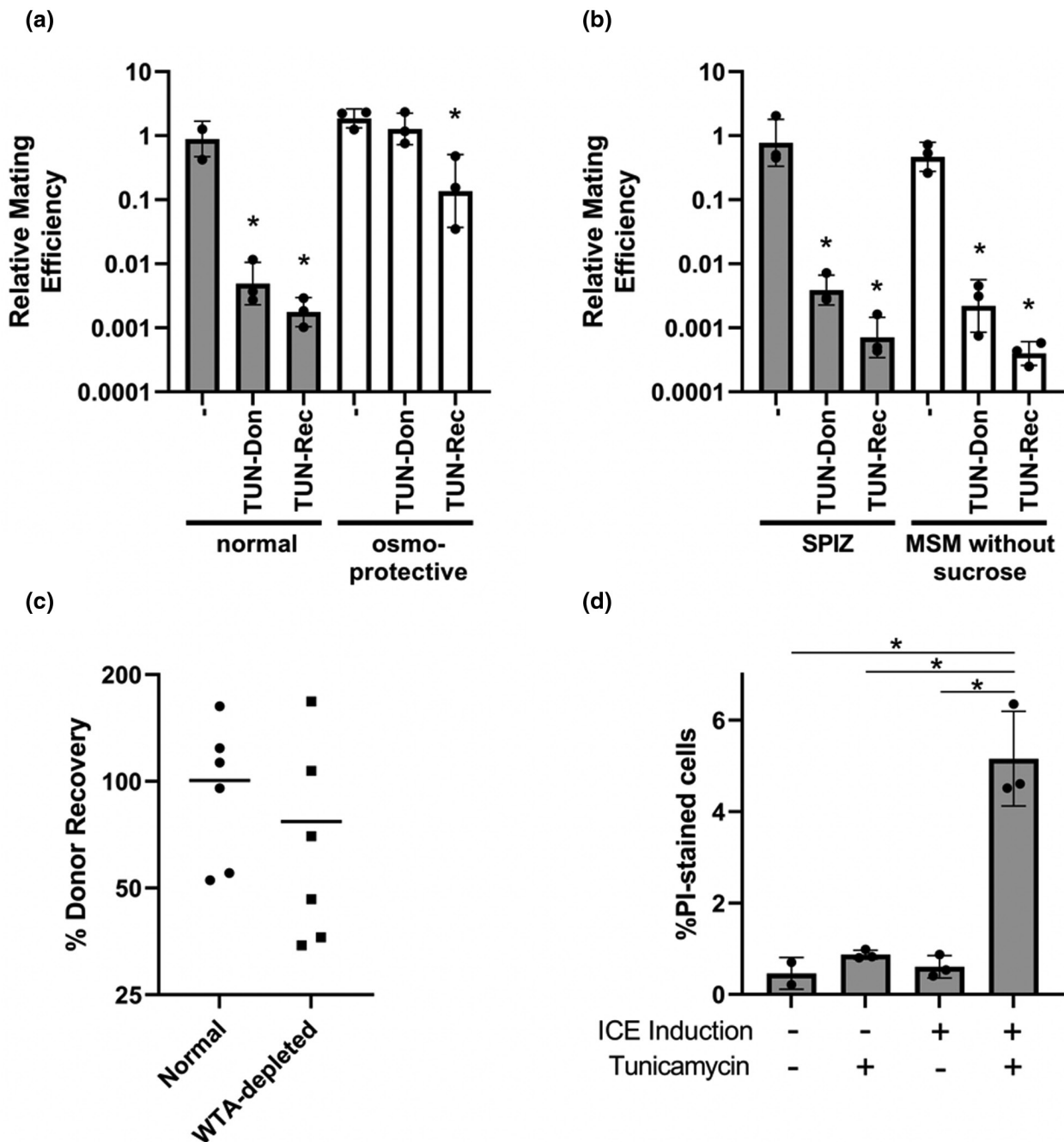
treatment with lysozyme and autolysins (Atilano et al., 2010; Bera et al., 2007; Tiwari et al., 2018).

Based on the role of WTAs in modulating the activity of cell wall hydrolases, we hypothesized that WTA-depleted cells might have cell walls that are more sensitive to the formation of mating pairs. If true, then the decrease in conjugation efficiency should be suppressed (conjugation restored) under osmoprotective conditions that would enable cells to survive severe defects in their walls.

We found that the conjugation defect of WTA-depleted ICEBs1 donors was completely suppressed when matings were done on an osmoprotective surface (Figure 4a). Matings were done on a standard mating surface (Spizizen's salts, described in Experimental Procedures) or an osmoprotective mating surface that contained 20mM MgCl$_2$ and 0.5 M sucrose, buffered with 20mM maleic acid pH 7 (MSM), an osmoprotective supplement that has been used to maintain protoplasts (lacking cell walls) and prevent bacterial cell death from osmotic stress (Leaver et al., 2009; Wyrick & Rogers, 1973). A deletion of a sucrose metabolism gene was incorporated into all strains used in these osmoprotection mating assays to prevent degradation of the sucrose osmoprotectant (Wolf et al., 2012). At the conclusion of the mating, cells were resuspended and diluted in MSM and then plated and grown on non-protective LB plates with the appropriate antibiotics to select for transconjugants.

As described above, treatment of donors with tunicamycin (1 μg/ml) for 60 min to deplete WTAs caused a mating defect under standard mating conditions (Figure 4a). In contrast, this defect was fully suppressed under osmoprotective conditions and mating efficiencies were indistinguishable from those of cells without tunicamycin treatment (Figure 4a).

Similarly, we found that the mating defect associated with WTA-depleted recipients was largely suppressed when matings were done on an osmoprotective mating surface (Figure 4a). There was still an approximately 5- to 10-fold drop in conjugation efficiency with WTA-depleted recipients on the osmoprotective mating surface relative to untreated cells (Figure 4a). This drop was likely due to death of transconjugants that did not sufficiently recover from cell wall damage before the shift to non-protective conditions (LB agar).

Suppression of the mating defect on the osmoprotective surface (MSM) was due to osmoprotection by sucrose and not an effect of MgCl$_2$ or the malate buffer. When sucrose was omitted from the mating surface, there was no rescue of the conjugation defect caused by depletion of WTAs (Figure 4b). These results support the model that WTA-depleted cells die from osmotic stress. Furthermore, we conclude that WTA-depleted donors have significantly decreased ability to transfer ICEBs1, perhaps because they die before they can successfully participate in conjugation. This could be due to overall death of all or the vast majority of ICEBs1-containing cells, or selective death of a subpopulation, perhaps those that form mating pairs with recipients.

2.7 | WTA-depleted cells in ICEBs1 mating pairs are more likely to die

We found that there was not a large decrease in the number of viable WTA-depleted donors during mating under standard

(non-osmoprotective) conditions. As above, ICEBs1 was activated and cells were simultaneously treated with tunicamycin. This tunicamycin treatment caused a mild (3.7-fold) decrease in CFUs relative to untreated cells (1.1×10^8 CFU/ml for untreated cells versus 3.0×10^7 CFU/ml). We suspect that this drop in CFUs following tunicamycin treatment was due, at least in part, to defects in cell separation after division. We combined these donors with an ICE^0 recipient on a (non-protective) mating surface. The percentage of viable donors recovered after mating was similar between cells with and without tunicamycin treatment (Figure 4c), although there appeared to be a small drop in recovery of the tunicamycin-treated cells. Based on these results, we conclude that there is not a large drop in viability of the population of donors.

This population-level observation from the conclusion of a mating protocol does not reflect what occurs at the single-cell level. Although the vast majority of ICEBs1-containing cells are potential donors, only a small number (~1%) successfully participate in conjugation under conditions used here. Based on the results above, we hypothesized that WTA-depleted donors that are part of a mating pair likely undergo cell death. This would represent death of a small fraction of the population that would not be readily observed by bulk population-based viability assays.

We used propidium iodide (PI) staining and fluorescence microscopy to monitor death (loss of cell envelope integrity) of single cells. We induced a population of ICEBs1 donors to mate, concentrated them at high density on an agar pad containing propidium iodide, and monitored the cells for 2 h, and counted the number of envelope-damaged (PI-stained) cells after 2 h. Because mating is ordinarily a rare event, we used a monoculture of ICEBs1 donors lacking the ICE gene yddJ, which encodes a protein that would normally block the ICE+ cell from serving as a recipient in a mating pair (Avello et al., 2019). This allowed all cells to potentially serve as donors and recipients, thereby significantly increasing the frequency of conjugation. When ICEBs1 was induced in WTA-depleted cells under these conditions, we observed an approximately eightfold increase in the incidence of PI-stained bacteria, indicating that WTA-depleted cells are more likely to die under conditions that support ICEBs1 transfer (Figures 4d and S2).

2.8 | The activity of the ICEBs1 conjugation machinery is sufficient to kill WTA-depleted donors and recipients

Our results indicate that WTA-depleted donors and recipients are defective in ICEBs1 mating due to envelope damage. In the case of matings using WTA-depleted recipients, this could be because (1) WTA-depleted recipients never acquire ICEBs1, likely because forming a mating pair is lethal to WTA-depleted cells, or because (2) WTA-depleted recipients acquire ICEBs1 and become transconjugants but subsequently die, perhaps due to the expression of ICEBs1 genes or the transconjugant becoming a new donor.

We found that transfer of ICE*Bs1* into WTA-depleted recipients was not required for the decrease in conjugation efficiency. We measured mobilization of the plasmid pC194 by the ICE*Bs1* conjugation machinery into WTA-depleted recipients. In these experiments, we used a mutant ICE*Bs1* that is unable to excise from the chromosome (Δ*attR*) and that lacks a functional origin of transfer (Δ*oriT*). When activated, this ICE mutant still expresses the conjugation machinery and is able to mobilize several plasmids that do not encode their own conjugation system, including pC194 (Lee et al., 2012). We activated ICE*Bs1* gene expression and measured mobilization of pC194 into recipient cells. There was a ~100-fold decrease in mobilization efficiency of pC194 into WTA-depleted (tunicamycin treated) recipients compared with untreated recipients (Figure 5). Based on these results, we conclude that the decrease in conjugation efficiency into WTA-depleted recipients is not due to transfer of ICE*Bs1* into recipients and subsequent death of the new transconjugant; rather, the defect is likely due to death of transconjugants caused by the formation of mating pairs or the act of transferring any DNA.
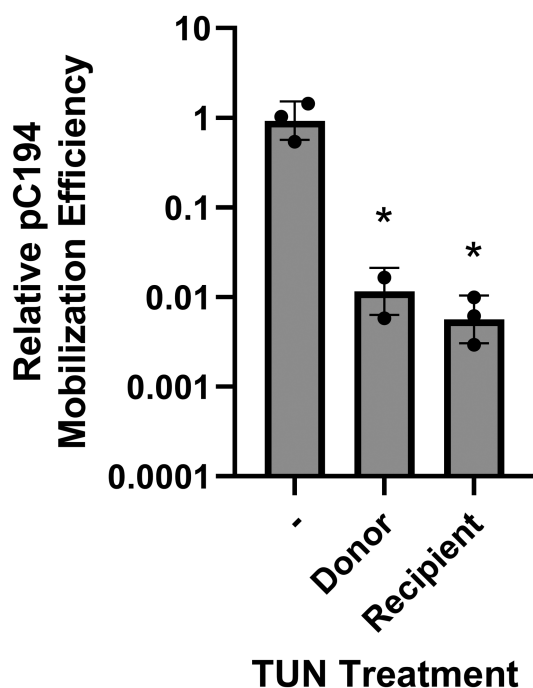
FIGURE 5 Mobilization of the non-conjugative plasmid pC194 by a locked-in ICE*Bs1* is negatively affected by WTA depletion. A strain containing both the mobilizable plasmid pC194 and a locked-in version of ICE*Bs1* (MMH868) was mated with an ICE*Bs1*[0] recipient strain (MMH676). WTAs were depleted in either the donor or recipient strain via treatment with 1 μg/ml tunicamycin for 60 min as in Figure 3a. Relative mobilization efficiency was calculated as the number of transconjugants (Cm[R] Strep[R] CFUs) per initial donor relative to an untreated control. Graphs shows averages and standard deviations of log-transformed data from three biological replicates. * indicates relative mobilization efficiency was significantly different from 1 (one-way ANOVA and Dunnett's multiple comparisons test, $p < .05$). Average mobilization efficiency of the untreated control was 1.4×10^{-3} with a standard deviation of 6.2×10^{-4}

We performed similar experiments with WTA-depleted donor cells in which ICE*Bs1* could not transfer, but the ICE-encoded conjugation machinery could mobilize pC194. Again, there was an ~100-fold decrease in mobilization efficiency as measured by acquisition of pC194 (Figure 5). These results indicate that WTA-depleted donors are defective in transfer. Together with the results above, we infer that this defect is due to donor cell death in mating pairs.

3 | DISCUSSION

We used a CRISPRi screen to identify essential genes in *B. subtilis* that are needed for efficient conjugation of ICE*Bs1*. We found that WTAs are necessary in both donor and recipient cells for efficient transfer of ICE*Bs1*. Under mating conditions, likely in mating pairs, there was significant death of WTA-depleted cells. Cell death and the need for WTAs for conjugation were reduced or eliminated when matings were done in osmoprotective conditions. Together, our results indicate that WTA-depleted cells fail to mate because they die from damage to their cell envelope.

The defect in conjugation of WTA-depleted cells was dependent on the ICE*Bs1* conjugation machinery, but did not depend on ICE*Bs1* DNA being transferred. We found that WTA-depleted cells were defective in transfer of a plasmid that normally can be transferred by the ICE*Bs1* conjugation machinery. In contrast, there was little or no defect in transfer of Tn*916*. These results indicate that the primary effect of WTAs is likely not to enable cell-cell contact (unless Tn*916* has some unknown function that does this). Rather, WTAs are important for proper function or control of the conjugation machinery, and that there is something fundamentally different about the activity of the ICE*Bs1* conjugation machinery compared with that of Tn*916* (see below).

3.1 | Possible mechanisms of conjugation-dependent toxicity in WTA-depleted cells

WTAs are important regulators of cell wall hydrolases across bacterial species, and WTA-depleted gram-positive bacteria have previously been demonstrated to be more sensitive to autolysin and lysozyme treatment (Brown et al., 2013). WTAs are also important for the proper localization of autolysins. Some *B. subtilis* cell wall hydrolases appear to be excluded from binding peptidoglycan decorated by WTAs, and the enzymes are mislocalized in the absence of WTAs (Kasahara et al., 2016; Yamamoto et al., 2008). It is possible that WTAs similarly regulate the activity of the bifunctional cell wall hydrolase CwlT that is encoded by ICE*Bs1*, and that mis-regulation of CwlT, perhaps in combination with mis-regulation of other cell wall hydrolases in WTA-depleted cells, causes the lethal envelope damage during conjugation. It is challenging to test the role of CwlT on conjugation efficiencies of WTA-depleted cells because *cwlT* is required for conjugation (DeWitt & Grossman, 2014).

WTAs also have a role in cell wall biosynthesis, and WTA-depleted *B. subtilis* cells exhibit irregularities in cell wall thickness and severe cell

shape defects (D'Elia et al., 2006). It is possible that WTA-depletion in *B. subtilis* results in an unusually fragile cell wall, and that WTA-depleted *B. subtilis* is consequently much more sensitive to the normal cell wall modification process that occurs during conjugation.

The strains investigated in this study were all derived from *B. subtilis* 168, which utilizes glycerol 3-phosphate-(GroP) based WTAs. In contrast, some bacteria utilize ribitol 3-phosphate- (RboP) based WTAs in lieu of GroP-based WTAs. Prior reports indicate that ICE*Bs1* is capable of efficient transfer into a wide variety of recipients, including *Listeria monocytogenes* (Auchtung et al., 2005; Brophy et al., 2018), which is reported to utilize RboP-based WTAs (Eugster & Loessner, 2011). ICE*Bs1* is also capable of transfer (albeit less efficiently) into *Staphylococcus aureus* (Brophy et al., 2018), which also utilizes RboP-based WTAs (Brown et al., 2013). Based on these results, we speculate that the requirement for WTAs in an ICE*Bs1* recipient is likely not specific to GroP-WTAs versus RboP-WTAs.

3.2 | Activity of the conjugation machinery

Our results have interesting implications concerning the activity of the conjugation machinery and its effects on donor and recipient cells. First, cell death of WTA-depleted donors occurs only during mating conditions, and in a small subpopulation of cells. This indicates that the conjugation machinery is only activated in the presence of recipients, likely only in mating pairs. This is consistent with analyses of other elements that indicate the conjugation machinery is activated by cell-cell contact [reviewed in: (Christie et al., 2014)].

Additionally, if the decrease in acquisition of ICE*Bs1* by WTA-depleted recipients is due to killing that is mediated by the ICE*Bs1*-encoded cell wall hydrolase CwlT, then this indicates that the donor-encoded hydrolase is acting on recipient cells. There are other interpretations of this result: for example, the WTA-depleted cell's own autolysins could be hyper-active, and active conjugation machinery from the donor could exacerbate the effects of hyper-active autolysins in recipients in mating pairs, thereby causing cell death.

Although CwlT is one possible cause of the conjugation-dependent toxicity among WTA-depleted cells, there are alternative explanations which cannot be ruled out. For example, WTA-depletion in *B. subtilis* sensitizes the cells to PBP-targeting antibiotic methicillin (Farha et al., 2013), and it is possible that the ICE*Bs1* conjugation machinery comparably interferes with cell wall biosynthesis in a way that is incompatible with WTA depletion. Alternatively, ICE*Bs1* conjugation could involve inactivating or modifying teichoic acids in a way that is lethal to WTA-depleted bacteria.

3.3 | Different ICEs respond differently to WTA depletion

We found that Tn*916* transfer was not negatively impacted by WTA-depletion, in contrast to our results with ICE*Bs1*. ICE*Bs1* and Tn*916* are closely related elements. The conjugation and replication machinery of ICE*Bs1* is homologous to that of Tn*916*, with common genes between the two elements having about 30% sequence identity (Churchward, 2008). Additionally, both elements have a modular organization, with genes related to conjugation, and regulation of activation organized into distinct groups (Burrus & Waldor, 2004). Like CwlT, the cell wall hydrolase encoded by Tn*916* (Orf14) is predicted to be a bifunctional hydrolase containing both muramidase and peptidase domains (Xu et al., 2014), and CwlT and Orf14 are about 43% identical.

An important difference between ICE*Bs1* and Tn*916* that might contribute to this observation is that transfer of Tn*916* is less efficient than that of ICE*Bs1*. It is possible that less conjugation machinery is made when Tn*916* becomes transcriptionally active, and therefore the formation of mating pairs is not as stressful with the Tn*916*-encoded conjugation machinery as it is with that from ICE*Bs1*. It is also possible that the relevant components of the Tn*916* conjugation machinery are not regulated by *B. subtilis* WTAs, perhaps reflective of the broad host range of Tn*916*. It remains to be determined what it is about the ICE*Bs1* and Tn*916*-encoded conjugation machineries that make them respond so differently to *B. subtilis* WTAs.

Recent studies of ICE*St3* of *Streptococcus thermophilus* found that deleting a *tagO*-like gene, which might result in a decrease in WTAs, resulted in complex effects on transfer efficiency. Deletion in donors caused a decrease, but deletion in recipients caused an increase in conjugation efficiency (Dahmane et al., 2018). It is not clear if these effects are alleviated by osmoprotective conditions and if they are related to the effects described here for ICE*Bs1*.

3.4 | Conjugation and cell envelope stress

Connections between conjugation and envelope stress have long been known. One classic example is in *E. coli* where excessive transfer of F plasmids into F- recipients can lead to death of the recipient, a phenomenon called lethal zygosis (Skurray & Reeves, 1973). Subsequent studies found that radiolabeled peptidoglycan components are released into the medium when lethal zygosis occurs, indicating that the mechanism of death is due to damage of the cell envelope (Ou, 1980). Furthermore, activation of the F-plasmid sensitizes cells to certain envelope-disrupting antimicrobials (i.e. bile salts) (Bidlack & Silverman, 2004). The F plasmid has also been demonstrated to encode the means to upregulate the cell envelope stress response pathway in the host bacterium, which likely helps protect host cells from envelope stress caused by the F-encoded conjugation machinery (Grace et al., 2015). Activation of ICE*Bs1* may also result in the upregulation of *liaH* (Auchtung et al., 2005), previously named *yvqH*, that encodes a homolog of phage shock protein A. *liaH* is activated by the LiaRS cell envelope response system and is thought to have a role in maintaining the integrity of the cell envelope, although its specific function is not well understood (Radeck et al., 2017).

Our results indicate that WTAs have an important role in protecting *B. subtilis* against envelope stress caused by the ICE*Bs1*

conjugation machinery. We suspect that WTAs in other gram-positive bacteria also have a role in conjugation, and that role very likely will depend on aspects of the specific conjugation machinery assembled in the cell envelope.

4 | EXPERIMENTAL PROCEDURES

4.1 | Media and growth conditions

B. subtilis strains were grown at 37°C with shaking in LB medium. Experimental cultures were started from 3 ml LB exponential phase cultures inoculated from a single colony.

Where needed, *B. subtilis* strains were grown in LB at the following antibiotic concentrations for selection or maintenance of marked alleles: kanamycin (5 μg/ml), streptomycin (100 μg/ml), spectinomycin (100 μg/ml), chloramphenicol (5 μg/ml), and a combination of erythromycin (0.5 μg/ml) and lincomycin (12.5 μg/ml) to select for macrolide-lincosamide-streptogramin (MLS) resistance and erythromycin resistance. Tunicamycin was used at 1 μg/ml to inhibit WTA synthesis.

The osmoprotective supplement MSM (0.5 M sucrose, 20 mM MgCl2, buffered with 20 mM maleic acid pH 7) (Leaver et al., 2009; Wyrick & Rogers, 1973) was used where indicated. It was added from a 2× stock.

4.2 | Strains and alleles

Escherichia coli strain AG1111 (MC1061 F' *lacI*q *lacZM15* Tn*10*) was used for routine cloning and plasmid construction.

The *B. subtilis* strains used in this study are listed in Table 1. Strains were constructed using natural transformation (Harwood & Cutting, 1990). All *B. subtilis* strains are derivates of JH642 and contain tryptophan and phenylalanine auxotrophies (*trpC2 pheA1*) (Brehm et al., 1973; Smith et al., 2014). Many of the alleles used in this study have been described previously and are briefly summarized below.

Donor strains used in standard ICE*Bs1* mating assays contained the allele Δ(*rapI-phrI)342::kan* (Auchtung et al., 2005). ICE*Bs1* was activated in donor strains by inducing expression of *rapI* from one of three promoter fusions: the LacI-repressible-IPTG-inducible promoters Pspank-*rapI* or Pspank(hy)-*rapI* (Auchtung et al., 2005), or the xylose-inducible promoter Pxyl-*rapI* (Berkmen et al., 2010). For the first two, *rapI* expression was induced by adding Isopropyl-β-D-thiogalactopyranoside (IPTG, Sigma) to a final concentration of 1 mM. Pxyl-*rapI* expression was induced via the addition of xylose to a final concentration of 1% w/v. ICE*Bs1*-containing strains used in live cell microscopy also contained a deletion of *yddJ* (Avello et al., 2019).

Recipient strains were derived from the ICE*Bs1*-cured (ICE*Bs1*⁰) strain JMA222 (Auchtung et al., 2005) and were streptomycin resistant (*str84*) to facilitate counterselection during mating experiments.

Recipient strains also contained *spc*-marked null alleles of competence genes *comK* or *comC* to prevent natural transformation.

ICE*Bs1* donor and recipient strains that were used in osmoprotective mating assays also contained a deletion-insertion of *sacB* (Δ*sacB::erm*) (Koo et al., 2017) to prevent degradation of sucrose (Wolf et al., 2012). A strain containing this allele was obtained from the Bacillus Genetic Stock Center (www.bgsc.org).

4.2.1 | *ycgO*::{Pspank-*rapI* (*spc*)}

We constructed a *spc*-marked Pspank-*rapI* allele integrated into the nonessential *B. subtilis* gene *ycgO*. We used a previously described Pspank-*rapI* (*spc*) allele as a template for PCR amplification (Auchtung et al., 2005). The amplified allele was joined with *ycgO* flanking sequences by isothermal assembly (Gibson et al., 2009), and the construct was introduced to wild type *B. subtilis* via natural transformation selecting for spectinomycin resistance.

4.2.2 | *comC*::*spc*

We constructed a *comC* deletion-insertion allele, extending from 324 bp upstream and 26 bp downstream of the *comC* open reading frame, with the *aad9* (*spc*) gene from pMagellan6. The allele was constructed by joining the appropriate *comC* flanking sequences with the amplified *aad9* gene by isothermal assembly, and was moved into wild type *B. subtilis* via natural transformation selecting for spectinomycin resistance.

4.2.3 | Δ*dltABCDE*::*cat*

We constructed a *dltABCDE* deletion-insertion allele: The deletion extends from 1 bp upstream of the *dltA* open reading frame to 22 bp upstream of the 3′ end of the *dltE* open reading frame, and *cat* from pGEMcat (Youngman et al., 1989) is inserted. The allele was constructed by joining the appropriate *dlt* operon flanking sequences with the amplified *cat* by isothermal assembly, and was introduced into wild type *B. subtilis* via natural transformation selecting for chloramphenicol resistance.

4.2.4 | Pspank-*tag* alleles

We constructed a set of three fusions that placed each of three endogenous WTA biosynthesis operons (*tagO*, *tagAB*, *tagDEF*) under the control of the IPTG-inducible promoter Pspank. In each case, Pspank was introduced upstream of the first gene in the operon by single crossover integration. We used a plasmid (pJCL86; lab collection) that contains Pspank and *lacI* inserted into the backbone of pAG58 (Jaacks et al., 1989). A short region of the 5′UTR encompassing the predicted ribosome binding site and a few hundred

Strain	Genotype[1] (reference)
CAL85	ICE*Bs1*[0] *str-84* (Lee et al., 2007)
CAL89	ICE*Bs1*[0] *str-84 comK::spc* (Auchtung et al., 2005)
CMJ253	ICE*Bs1*[0] Tn*916*+ (Johnson & Grossman, 2014)
CAL874	ICE*Bs1* Δ(*rapI-phrI*)*342::kan amyE::(Pxyl-rapI spc)* (Lee et al., 2010)
MMH211	ICE*Bs1* Δ(*rapI-phrI*)::(*kan amyE*) Δ*amyE117::(Pspank-rapI spc) lacA::(Pxyl-dcas9 spc)*
MMH233	ICE*Bs1* Δ(*rapI-phrI*)::{*kan amyE::(Pveg-sgRNA*[cgeD] *cat*)} Δ*amyE117::(Pspank-rapI spc) lacA::(Pxyl-dcas9 spc)*
MMH525	ICE*Bs1* Δ(*rapI-phrI*)*342::kan ycgO::(Pspank-rapI spc) amyE::(Pveg-sgRNA*[cgeD] *cat) lacA::(Pxyl-dcas9 spc)*
MMH527	ICE*Bs1* Δ(*rapI-phrI*)*342::kan ycgO::(Pspank-rapI spc) amyE::(Pveg-sgRNA*[tagA] *cat) lacA::(Pxyl-dcas9 spc)*
MMH541	ICE*Bs1* Δ(*rapI-phrI*)*342::kan amyE::(Pxyl-rapI spc)* Δ*dltABCDE::cat*
MMH545	ICE*Bs1*[0] *str-84* Δ*dltABCDE::cat*
MMH550	ICE*Bs1* Δ(*rapI-phrI*)*342::kan ycgO::(Pspank-rapI spc)*
MMH577	ICE*Bs1* Δ(*rapI-phrI*)*342::kan amyE::(Pxyl-rapI spc) tagO::(Pspank-tagO cat)*
MMH578	ICE*Bs1* Δ(*rapI-phrI*)*342::kan amyE::(Pxyl-rapI spc) tagA::(Pspank-tagA cat)*
MMH584	ICE*Bs1*[0] *str-84 tagA::(Pspank-tagA cat)*
MMH608	ICE*Bs1* Δ(*rapI-phrI*)*342::kan amyE::(Pxyl-rapI spc) tagD::(Pspank-tagD cat)*
MMH676	ICE*Bs1*[0] *str-84 comC::spc*
MMH788	ICE*Bs1* Δ*yddJ* Δ(*rapI-phrI*)*342::kan*
MMH794	ICE*Bs1* Δ*yddJ* Δ(*rapI-phrI*)*342::kan amyE::(Pspank(hy)-rapI spc)*
MMH797	ICE*Bs1*[0] *str-84 comC::spc sacB::mls*
MMH862	ICE*Bs1* Δ(*rapI-phrI*)*342::kan ycgO::(Pspank-rapI spc) sacB::mls*
MMH868	ICE*Bs1* Δ*oriT285* Δ(*rapI-phrI*)*342::kan* Δ*attR::mls ycgO::(Pspank-rapI spc)* pC194(*cat*)

[1]All strains are derived from lab strain AG174 (JH642) (Brehm et al., 1973; Smith et al., 2014) and contain the *trpC2* and *pheA1* alleles (not show).

bp of the 5′ region of the ORFs of *tagO*, *tagA*, and *tagD* were each amplified from wild type *B. subtilis* genomic DNA. The region amplified from each gene corresponded to the following: 19 bp upstream to 357 bp downstream of the *tagO* translation start site, 24 bp upstream to 277 bp downstream of the *tagA* translation start site, and 25 bp upstream to 157 bp downstream of the *tagD* translation start site. Each segment was inserted between the SphI and HindIII sites of pJCL86 via isothermal assembly, yielding plasmids pMMH558 (*tagO*), pMMH559 (*tagA*), and pMMH605 (*tagD*). The plasmids were transformed into wild type *B. subtilis* selecting for chloramphenicol resistance in the presence of 1 mM IPTG. Proper integration of each plasmid was confirmed by diagnostic PCR and DNA (Sanger) sequencing. The resulting *B. subtilis* strains grew normally in the presence of 1 mM IPTG and exhibited severe growth defects in the absence of IPTG. Briefly, the Pspank-*tag* strains were grown in medium containing 1 mM IPTG and then transitioned into growth medium containing different IPTG concentrations (100 μM, 20μM, 10 μM, or 0 μM IPTG). Strains were grown in the reduced IPTG concentration for approximately six generations and were subsequently analyzed by light microscopy.

All Pspank-*tag* strains exhibited the distinctive cell shape and separation defects characteristic of *B. subtilis* cells depleted of WTAs (D'Elia et al., 2006) when grown in medium containing 20 μM, 10 μM, or 0 μM IPTG (Figure S1).

4.2.5 | Construction of strains for mobilization of pC194

We constructed a *B. subtilis* strain containing the plasmid pC194 and a mutant of ICE*Bs1* that is unable to excise (Δ*attR*, "locked-in") and without a functional origin of transfer (Δ*oriT*). This strain was made by moving the *ycgO*::{Pspank-*rapI* (*spc*)} allele into the ICE*Bs1*[0] strain JMA222, creating strain MMH863. A version of ICE*Bs1* containing three mutations, Δ(*rapI-phrI*)*342::kan*, Δ*oriT*, and Δ*attR::mls*, was moved into MMH863 via natural transformation, and pC194 was subsequently introduced via natural transformation. The unmarked *oriT* deletion in this element has been described (Jones et al., 2021). The Δ*attR::mls* allele was constructed via isothermal assembly using *mls* from pCAL215 (Lee et al., 2007) as a template, and has the same

deletion boundaries as a previously reported Δ*attR*::*tet* allele (Lee & Grossman, 2007).

4.2.6 | Construction of CRISPRi ICE*Bs1* donor library

The Pxyl-*dcas9* and Pveg-*sgRNA* alleles used to generate the CRISPRi knockdown library of ICE*Bs1* donor strains were previously described and a generous gift from Peters et al. (2016). The library of sgRNAs used in this study (a gift of Peters et al.) collectively targeted a set of 289 proposed essential *B. subtilis* genes (Peters et al., 2016), 257 of which were subsequently verified to be essential in a systematic gene knockout analysis (Koo et al., 2017). The initial library contains a set of 299 plasmids, each containing a Pveg-*sgRNA* allele with a unique 20 bp targeting region, a *cat* marker conferring chloramphenicol resistance, and the appropriate flanking homology needed to integrate the sgRNA allele into the *B. subtilis* chromosome at *amyE* via double crossover. We utilized a pooled collection of these plasmids to generate our library of Pveg-*sgRNA* alleles integrated into ICE*Bs1*.

Our strategy was to insert *amyE* into ICE*Bs1*, delete *amyE* from the chromosome, and then recombine the Pveg-*sgRNA* library into *amyE* in ICE*Bs1*. We constructed a deletion-insertion of *amyE* (Δ*amyE117*::{Pspank-*rapI* (*spc*)}) that replaces the entire chromosomal gene and flanking noncoding regions with Pspank-*rapI*. This allele was constructed using a previously described Pspank-*rapI* (*spc*) allele (Auchtung et al., 2005) as a template for PCR amplification, and by joining the amplified product to *amyE* flanking homology via isothermal assembly. The construct was transformed into *B. subtilis* selecting for resistance to spectinomycin. The allele was confirmed by sequencing PCR-amplified DNA and verified functionally to activate ICE*Bs1* following addition of IPTG.

We used isothermal assembly to construct a *kan*-marked copy of *amyE* with flanking sequences needed to integrate the allele into *rapI-phrI* of ICE*Bs1*. This allele (Δ(*rapI-phrI*)::{*amyE kan*}) was designed such that the deletion boundaries and orientation of the *kan* cassette would be identical to Δ(*rapI-phrI*)*342*::*kan*.

The pooled library of Pveg-*sgRNA* plasmids was linearized with KpnI-HF (NEB), and was incorporated into the ICE::*amyE* locus by transformation into strain MMH211 and selecting for resistance to chloramphenicol. We recovered ≥1.5 ×10^5 transformants in total. Transformants were resuspended and pooled in MOPS-buffered S7$_{50}$ defined minimal medium (Jaacks et al., 1989) lacking a carbon source (1× S7$_{50}$ + metals) and frozen in aliquots for future use.

We constructed one Pveg-*sgRNA* allele for use as a control, with a 20 bp targeting region corresponding to the nonessential *B. subtilis* gene *cgeD*. To construct this allele we used inverse PCR as previously described (Larson et al., 2013) using pJMP2 as a template for amplification (Peters et al., 2016), creating plasmid pMMH221. The plasmid was linearized with KpnI-HF and transformed into the appropriate *B. subtilis* strains via selection with chloramphenicol. A copy of ICE*Bs1* with the Pveg-*sgRNA*^{cgeD} allele incorporated into the ICE::*amyE* integration site was confirmed to transfer normally.

4.3 | CRISPRi library mating

We used the CRISPRi system in ICE*Bs1* to partially decrease expression of essential genes in the ICE*Bs1* donor library. We used partial rather than full expression of *dcas9* because pilot experiments with maximal expression indicated that full expression of *dcas9* (1% xylose) in combination with an sgRNA targeting an essential gene caused a significant fitness defect in many donor library strains that would strongly bias or interfere with the screen. Similarly, we opted not to use leaky expression of *dcas9* (0% xylose) because pilot experiments suggested that the knockdowns would not be strong enough to generate notable variations in sgRNA allele frequency in the resulting transconjugant population.

A lawn of the CRISPRi ICE*Bs1* donor library was started from freezer stocks on the day before the experiment and grown overnight at room temperature on an LB plate. The following day, the lawn was used to start a culture at OD600 = 0.02 in LB supplemented with 0.01% xylose to stimulate transcription of Pxyl-*dcas9* and with kanamycin to ensure maintenance of the *kan*-marked ICE*Bs1*. When cultures reached an OD600 of 0.15, ICE*Bs1* was activated by addition of IPTG (1 mM) for 1 h to induce expression of Pspank-*rapI*.

Mating of the library into the streptomycin-resistant, ICE-cured recipient strain CAL89 was conducted using a standard mating procedure (see below). An aliquot of the donor culture was harvested for analysis immediately prior to mixing donors and recipients. At the conclusion of the mating, the cells on the filter were resuspended and plated on LB agar containing kanamycin and streptomycin to select for transconjugants and incubated overnight at 37°C. Transconjugants were then resuspended in 1× S7$_{50}$ + metals and pooled, and an aliquot of the resuspension was harvested for sequence analysis.

4.4 | Amplification and sequencing of pooled sgRNA alleles

We used Qiagen DNeasy Blood and Tissue kits to extract DNA from the pre- and post-mating samples, following the manufacturer instructions for the use of the kit with gram-positive bacteria. We used KAPA HiFi MasterMix to amplify the genes encoding the sgRNA from the DNA samples, adhering to the manufacturer protocol. We used 300 ng of sample DNA as a template and ran the reactions for 20 PCR cycles. The primers used to amplify the sgRNA alleles were oMH238 (5′-AATGATACGGCGACCACCGAGATCTACACGGGCGGGAATGGGCTCGTGTTGTACAATAAATGT-3′) and oMH239 (5′-CAAGCAGAAGACGGCATACGAGATXXXXXXGCCAGCCGATCCTCTTCTGAGATGAGTTTTTGTTCG-3′). The 5′ ends of these oligos encode the Illumina adaptor sequences, and the X's correspond to multiplexing barcodes. The resulting amplicons were purified with SureSelect AMPure beads according to manufacturer instructions. DNA quality was checked with a bioanalyzer. Indexed samples were pooled and sequenced at the MIT BioMicro Center. The variable regions of the sgRNA amplicons

were sequenced with an Illumina MiSeq, using a 20 bp read length and primer oMH240 (5′-GGGCGGGAATGGGCTCGTGTTGTACA ATAAATGT-3′) to sequence the variable region of the sgRNA allele and oMH241 (5′-CGAACAAAAACTCATCTCAGAAGAGGA TCGGCTGGC-3′) to sequence the multiplexing barcode. FastQC (version 0.11.5) was used to assess quality of raw sequences. The 20 nt reads were matched to the respective variable regions from the sgRNA library using the R (version 3.4.4) package ShortRead, with allowance for up to 2 mismatches per read. Raw sequencing data are available at the Sequence Read Archive (accession numbers SAMN25690317 and SAMN25690318 for the donor and transconjugant read data, respectively).

4.5 | Mating assays

Mating assays were conducted as previously described (Auchtung et al., 2005; DeWitt & Grossman, 2014; Johnson & Grossman, 2014), with minor modifications. Experimental cultures of donor and recipient strains were started in LB at an OD600 of 0.02 and grown with shaking at 37°C. Kanamycin was added to cultures of strains containing a *kan*-marked ICE*Bs1* to ensure maintenance of the element. ICE*Bs1* activation was induced via overexpression of *rapI*, at an OD600 of 0.15 in donor cultures by adding either 1mM IPTG (to induce expression of Pspank-*rapI* or Pspank(hy)-*rapI*) or 1% xylose (to induce expression of Pxyl-*rapI*). One hour after induction, 2.5 OD600 equivalents of donors were combined with an equal amount of recipients. The mixture of donors and recipients was collected on an nitrocellulose filter via vacuum filtration and washed with 5 ml 1× Spizizen's salts (2 g/L $(NH_4)SO_4$, 14 g/L K_2HPO_4, 6 g/L KH_2PO_4, 1 g/L Na_3 citrate-$2H_2O$, and 0.2 g/L $MgSO_4$-$7H_2O$) (Harwood & Cutting, 1990). The filter was placed on a 1× Spizizen's salts 1.5% agar plate (without a carbon source) and incubated at 37°C for 2 h. The cells were resuspended in 5 ml 1× Spizizen's salts. Transconjugants were quantified by serially diluting the resuspension in 1× Spizizen's salts, spreading the cells on an LB 1.5% agar plate containing kanamycin and streptomycin (for ICE*Bs1* matings), and incubating the plates overnight at 37°C. Donors were quantified immediately prior to combining donor and recipient cells: an aliquot of the donor culture was serially diluted and plated on an LB 1.5% agar plate containing kanamycin and grown overnight at 37°C. Mating efficiency was calculated as the number of transconjugants (kanamycin- and streptomycin-resistant post-mating CFUs/ml) per initial donor (pre-mating donor CFUs/ml). Data reported are normalized to the mean mating efficiency of a wild type control strain.

For mating assays done with individual strains with inducible CRISPRi-mediated knockdowns, Pxyl-*dcas9* expression was stimulated at the time of culture inoculation by supplementing the experimental cultures with 0.01% or 0.1% xylose.

For mating assays with strains in which the endogenous *tag* operons had been placed under the control of the IPTG-inducible

promoter Pspank, the LB starter cultures were grown in the presence of 100 μM IPTG. The starter cultures were pelleted by centrifugation and washed twice with plain LB (no IPTG). Cells were resuspended in LB containing the indicated concentration of IPTG (ranging from 0 to 100 μM), and were used to inoculate LB cultures containing IPTG at the same concentration. LB agar plates were supplemented with 1mM IPTG to obtain CFUs for strains with an IPTG-inducible promoter fused to an essential gene.

For mating assays with tunicamycin-treated strains, tunicamycin was added concurrently with ICE*Bs1* induction to a final concentration of 1 μg/ml.

For mating assays with Tn*916*, ICE activation was stimulated with 2.5 μg/ml tetracycline, and tetracycline was used in the selection for donors and transconjugants (instead of kanamycin).

For mating assays done on an osmoprotective mating surface, the 1× Spizizen's salts 1.5% agar plate was substituted for a 1× MSM 1.5% agar plate, and the cells were resuspended and diluted post-mating in 1× MSM instead of 1× Spizizen's salts. Pre- and post-mating CFUs were grown out by plating on non-osmoprotective LB 1.5% agar plates as described above. Sucrose was omitted from the 1× MSM solid and liquid media for the relevant experimental controls.

4.6 | pC194 mobilization assays

pC194 mobilization assays were carried out in essentially the same manner as ICE*Bs1* mating assays. Donor cultures were grown with chloramphenicol instead of kanamycin to maintain pC194 (containing *cat*). Donors and transconjugants were measured by plating on appropriate selective media.

4.7 | Live cell microscopy

Live cell microscopy was done largely as previously described (Babic et al., 2011) with minor modifications. Cultures of ICE*Bs1*+ Δ*yddJ* strains were grown in LB as described above. Strains either did or did not contain *amyE*::Pspank(hy)-*rapI*. All strains were treated with 1mM IPTG for 1 h at an OD600 of 0.15. For WTA-depletion, tunicamycin (1 μg/ml) was added concurrently with IPTG. After 1 h, cells were pelleted in a tabletop centrifuge at 14,000 rpm, washed once in 1× S750 + metals, and resuspended in 50 μl 1× S750 + metals. One microliter of the resuspension was applied to an agar pad. The agar pad comprised 1.5% Noble Agar (Difco) dissolved in carbonless 1.5% 1× S750 + metals medium and contained 30 μM propidium iodide.

The agar pad was placed on a glass coverslip (VWR) such that the cells would be in contact with the coverslip, and the coverslip was attached to a microscope slide via a frame-seal slide chamber (Bio-Rad). The cells were observed via a Nikon Ti-E inverted microscope and using a CoolSnap HQ camera (Photometrics). Propidium iodide fluorescence was generated with a Nikon Intensilight mercury illuminator

through an excitation and emission filter (Chroma; filter set 49008). The cells were monitored for PI-staining at 37°C for 2 h at 15 min timepoints. Image processing was carried out using ImageJ software. PI-stained cells from the final 2 h timepoint were quantified manually. At least 1000 cells were monitored for each biological replicate.

CONFLICT OF INTEREST

The authors declare no conflict of interest.

DATA AVAILABILITY STATEMENT

The data that support the findings of this study are available from the corresponding author upon reasonable request.

ORCID

M. Michael Harden https://orcid.org/0000-0002-6390-6008
Mary E. Anderson https://orcid.org/0000-0002-6930-3830
Alan D. Grossman https://orcid.org/0000-0002-8235-7227

REFERENCES

Allison, S.E., D'Elia, M.A., Arar, S., Monteiro, M.A. & Brown, E.D. (2011) Studies of the genetics, function, and kinetic mechanism of TagE, the wall teichoic acid glycosyltransferase in *Bacillus subtilis* 168. *Journal of Biological Chemistry*, 286, 23708–23716.

Arends, K., Celik, E.-K., Probst, I., Goessweiner-Mohr, N., Fercher, C., Grumet, L. et al. (2013) TraG encoded by the pIP501 type IV secretion system is a two-domain peptidoglycan-degrading enzyme essential for conjugative transfer. *Journal of Bacteriology*, 195, 4436–4444.

Atilano, M.L., Pereira, P.M., Yates, J., Reed, P., Veiga, H., Pinho, M.G. et al. (2010) Teichoic acids are temporal and spatial regulators of peptidoglycan cross-linking in *Staphylococcus aureus*. *Proceedings of the National Academy of Sciences of the United States of America*, 107, 18991–18996.

Auchtung, J.M., Aleksanyan, N., Bulku, A. & Berkmen, M.B. (2016) Biology of ICE*Bs1*, an integrative and conjugative element in *Bacillus subtilis*. *Plasmid*, 86, 14–25.

Auchtung, J.M., Lee, C.A., Monson, R.E., Lehman, A.P. & Grossman, A.D. (2005) Regulation of a *Bacillus subtilis* mobile genetic element by intercellular signaling and the global DNA damage response. *Proceedings of the National Academy of Sciences of the United States of America*, 102, 12554–12559.

Avello, M., Davis, K.P. & Grossman, A.D. (2019) Identification, characterization and benefits of an exclusion system in an integrative and conjugative element of *Bacillus subtilis*. *Molecular Microbiology*, 112, 1066–1082.

Babic, A., Berkmen, M.B., Lee, C.A. & Grossman, A.D. (2011) Efficient gene transfer in bacterial cell chains. *mBio*, 2, e00027-11.

Bantwal, R., Bannam, T.L., Porter, C.J., Quinsey, N.S., Lyras, D., Adams, V. et al. (2012) The peptidoglycan hydrolase TcpG is required for efficient conjugative transfer of pCW3 in *Clostridium perfringens*. *Plasmid*, 67, 139–147.

Bañuelos-Vazquez, L.A., Torres Tejerizo, G. & Brom, S. (2017) Regulation of conjugative transfer of plasmids and integrative conjugative elements. *Plasmid*, 91, 82–89.

Bera, A., Biswas, R., Herbert, S., Kulauzovic, E., Weidenmaier, C., Peschel, A. et al. (2007) Influence of wall teichoic acid on lysozyme resistance in *Staphylococcus aureus*. *Journal of Bacteriology*, 189, 280–283.

Berkmen, M.B., Lee, C.A., Loveday, E.-K. & Grossman, A.D. (2010) Polar positioning of a conjugation protein from the integrative and conjugative element ICE*Bs1* of *Bacillus subtilis*. *Journal of Bacteriology*, 192, 38–45.

Bhatty, M., Laverde Gomez, J.A. & Christie, P.J. (2013) The expanding bacterial type IV secretion lexicon. *Research in Microbiology*, 164, 620–639.

Bidlack, J.E. & Silverman, P.M. (2004) An active type IV secretion system encoded by the F plasmid sensitizes *Escherichia coli* to bile salts. *Journal of Bacteriology*, 186, 5202–5209.

Bonnet, J., Durmort, C., Mortier-Barrière, I., Campo, N., Jacq, M., Moriscot, C. et al. (2018) Nascent teichoic acids insertion into the cell wall directs the localization and activity of the major pneumococcal autolysin LytA. *Cell Surface*, 2, 24–37.

Bose, B., Auchtung, J.M., Lee, C.A. & Grossman, A.D. (2008) A conserved anti-repressor controls horizontal gene transfer by proteolysis. *Molecular Microbiology*, 70, 570–582.

Brehm, S.P., Staal, S.P. & Hoch, J.A. (1973) Phenotypes of pleiotropic-negative sporulation mutants of *Bacillus subtilis*. *Journal of Bacteriology*, 115, 1063–1070.

Brophy, J.A.N., Triassi, A.J., Adams, B.L., Renberg, R.L., Stratis-Cullum, D.N., Grossman, A.D. et al. (2018) Engineered integrative and conjugative elements for efficient and inducible DNA transfer to undomesticated bacteria. *Nature Microbiology*, 3, 1043–1053.

Brown, S., Santa Maria, J.P. & Walker, S. (2013) Wall teichoic acids of gram-positive bacteria. *Annual Review of Microbiology*, 67, 313–336.

Burrus, V. & Waldor, M.K. (2004) Shaping bacterial genomes with integrative and conjugative elements. *Research in Microbiology*, 155, 376–386.

Campbell, J., Singh, A.K., Santa Maria, J.P., Kim, Y., Brown, S., Swoboda, J.G. et al. (2011) Synthetic lethal compound combinations reveal a fundamental connection between wall teichoic acid and peptidoglycan biosyntheses in *Staphylococcus aureus*. *ACS Chemical Biology*, 6, 106–116.

Celli, J. & Trieu-Cuot, P. (1998) Circularization of Tn*916* is required for expression of the transposon-encoded transfer functions: characterization of long tetracycline-inducible transcripts reading through the attachment site. *Molecular Microbiology*, 28, 103–117.

Christie, P.J., Korman, R.Z., Zahler, S.A., Adsit, J.C. & Dunny, G.M. (1987) Two conjugation systems associated with *Streptococcus faecalis* plasmid pCF10: identification of a conjugative transposon

that transfers between *S. faecalis* and *Bacillus subtilis*. *Journal of Bacteriology*, 169, 2529–2536.

Christie, P.J., Whitaker, N. & González-Rivera, C. (2014) Mechanism and structure of the bacterial type IV secretion systems. *Biochimica et Biophysica Acta*, 1843, 1578–1591.

Churchward, G. (2008) Back to the future: the new ICE age. *Molecular Microbiology*, 70, 554–556.

D'Elia, M.A., Henderson, J.A., Beveridge, T.J., Heinrichs, D.E. & Brown, E.D. (2009) The N-acetylmannosamine transferase catalyzes the first committed step of teichoic acid assembly in *Bacillus subtilis* and *Staphylococcus aureus*. *Journal of Bacteriology*, 191, 4030–4034.

D'Elia, M.A., Millar, K.E., Beveridge, T.J. & Brown, E.D. (2006) Wall teichoic acid polymers are dispensable for cell viability in *Bacillus subtilis*. *Journal of Bacteriology*, 188, 8313–8316.

D'Elia, M.A., Millar, K.E., Bhavsar, A.P., Tomljenovic, A.M., Hutter, B., Schaab, C. et al. (2009) Probing teichoic acid genetics with bioactive molecules reveals new interactions among diverse processes in bacterial cell wall biogenesis. *Chemical Biology*, 16, 548–556.

Dahmane, N., Robert, E., Deschamps, J., Meylheuc, T., Delorme, C., Briandet, R. et al. (2018) Impact of cell surface molecules on conjugative transfer of the integrative and conjugative element ICE*St3* of *Streptococcus thermophilus*. *Applied and Environmental Microbiology*, 84, e02109-17.

Delavat, F., Miyazaki, R., Carraro, N., Pradervand, N. & van der. Meer, J.R. (2017) The hidden life of integrative and conjugative elements. *FEMS Microbiology Reviews*, 41, 512–537.

DeWitt, T. & Grossman, A.D. (2014) The bifunctional cell wall hydrolase CwlT is needed for conjugation of the integrative and conjugative element ICE*Bs1* in *Bacillus subtilis* and *B. anthracis*. *Journal of Bacteriology*, 196, 1588–1596.

Eugster, M.R. & Loessner, M.J. (2011) Rapid analysis of *Listeria monocytogenes* cell wall teichoic acid carbohydrates by ESI-MS/MS. *PLoS ONE*, 6, e21500.

Farha, M.A., Leung, A., Sewell, E.W., D'Elia, M.A., Allison, S.E., Ejim, L. et al. (2013) Inhibition of WTA synthesis blocks the cooperative action of PBPs and sensitizes MRSA to β-lactams. *ACS Chemical Biology*, 8, 226–233.

Frankel, M.B. & Schneewind, O. (2012) Determinants of murein hydrolase targeting to cross-wall of *Staphylococcus aureus peptidoglycan*. *Journal of Biological Chemistry*, 287, 10460–10471.

Frost, L.S., Leplae, R., Summers, A.O. & Toussaint, A. (2005) Mobile genetic elements: the agents of open source evolution. *Nature Reviews Microbiology*, 3, 722–732.

Gibson, D.G., Young, L., Chuang, R.-Y., Venter, J.C., Hutchison, C.A. & Smith, H.O. (2009) Enzymatic assembly of DNA molecules up to several hundred kilobases. *Nature Methods*, 6, 343–345.

Grace, E.D., Gopalkrishnan, S., Girard, M.E., Blankschien, M.D., Ross, W., Gourse, R.L. et al. (2015) Activation of the σE-dependent stress pathway by conjugative TraR may anticipate conjugational stress. *Journal of Bacteriology*, 197, 924–931.

Gross, M., Cramton, S.E., Götz, F. & Peschel, A. (2001) Key role of teichoic acid net charge in *Staphylococcus aureus* colonization of artificial surfaces. *Infection and Immunity*, 69, 3423–3426.

Guglielmini, J., Quintais, L., Garcillán-Barcia, M.P., de la Cruz, F. & Rocha, E.P.C. (2011) The repertoire of ICE in prokaryotes underscores the unity, diversity, and ubiquity of conjugation. *PLOS Genetics*, 7, e1002222.

Harwood, C.R. & Cutting, S.M. (1990) *Molecular biological methods for Bacillus*. Chichester, UK: John Wiley & Sons.

Jaacks, K.J., Healy, J., Losick, R. & Grossman, A.D. (1989) Identification and characterization of genes controlled by the sporulation-regulatory gene *spo0H* in *Bacillus subtilis*. *Journal of Bacteriology*, 171, 4121–4129.

Johnson, C.M. & Grossman, A.D. (2014) Identification of host genes that affect acquisition of an integrative and conjugative element in *Bacillus subtilis*. *Molecular Microbiology*, 93, 1284–1301.

Johnson, C.M. & Grossman, A.D. (2015) Integrative and conjugative elements (ICEs): what they do and how they work. *Annual Review of Genetics*, 49, 577–601.

Jones, J.M., Grinberg, I., Eldar, A. & Grossman, A.D. (2021) A mobile genetic element increases bacterial host fitness by manipulating development. *bioRxiv*, 10, e65924.

Kasahara, J., Kiriyama, Y., Miyashita, M., Kondo, T., Yamada, T., Yazawa, K. et al. (2016) Teichoic acid polymers affect expression and localization of dl-endopeptidase LytE required for lateral cell wall hydrolysis in *Bacillus subtilis*. *Journal of Bacteriology*, 198, 1585–1594.

Koo, B.-M., Kritikos, G., Farelli, J.D., Todor, H., Tong, K., Kimsey, H. et al. (2017) Construction and analysis of two genome-scale deletion libraries for *Bacillus subtilis*. *Cell Systems*, 4, 291–305.e7.

Larson, M.H., Gilbert, L.A., Wang, X., Lim, W.A., Weissman, J.S. & Qi, L.S. (2013) CRISPR interference (CRISPRi) for sequence-specific control of gene expression. *Nature Protocols*, 8, 2180–2196.

Laverde Gomez, J.A., Bhatty, M. & Christie, P.J. (2014) PrgK, a multidomain peptidoglycan hydrolase, is essential for conjugative transfer of the pheromone-responsive plasmid pCF10. *Journal of Bacteriology*, 196, 527–539.

Leaver, M., Domínguez-Cuevas, P., Coxhead, J.M., Daniel, R.A. & Errington, J. (2009) Life without a wall or division machine in *Bacillus subtilis*. *Nature*, 457, 849–853.

Lee, C.A., Auchtung, J.M., Monson, R.E. & Grossman, A.D. (2007) Identification and characterization of *int* (integrase), *xis* (excisionase) and chromosomal attachment sites of the integrative and conjugative element ICE*Bs1* of *Bacillus subtilis*. *Molecular Microbiology*, 66, 1356–1369.

Lee, C.A., Babic, A. & Grossman, A.D. (2010) Autonomous plasmid-like replication of a conjugative transposon. *Molecular Microbiology*, 75, 268–279.

Lee, C.A. & Grossman, A.D. (2007) Identification of the origin of transfer (*oriT*) and DNA relaxase required for conjugation of the integrative and conjugative element ICE*Bs1* of *Bacillus subtilis*. *Journal of Bacteriology*, 189, 7254–7261.

Lee, C.A., Thomas, J. & Grossman, A.D. (2012) The *Bacillus subtilis* conjugative transposon ICE*Bs1* mobilizes plasmids lacking dedicated mobilization functions. *Journal of Bacteriology*, 194, 3165–3172.

Leonetti, C.T., Hamada, M.A., Laurer, S.J., Broulidakis, M.P., Swerdlow, K.J., Lee, C.A. et al. (2015) Critical components of the conjugation machinery of the integrative and conjugative element ICE*Bs1* of *Bacillus subtilis*. *Journal of Bacteriology*, 197, 2558–2567.

Mirouze, N., Ferret, C., Cornilleau, C. & Carballido-López, R. (2018) Antibiotic sensitivity reveals that wall teichoic acids mediate DNA binding during competence in *Bacillus subtilis*. *Nature Communications*, 9, 5072.

Neuhaus, F.C. & Baddiley, J. (2003) A continuum of anionic charge: structures and functions of d-alanyl-teichoic acids in gram-positive bacteria. *Microbiology and Molecular Biology Reviews*, 67, 686–723.

Ou, J.T. (1980) Role of surface exclusion genes in lethal zygosis in *Escherichia coli* K12 mating. *Molecular Genetics and Genomics*, 178, 573–581.

Perego, M., Glaser, P., Minutello, A., Strauch, M.A., Leopold, K. & Fischer, W. (1995) Incorporation of D-alanine into lipoteichoic acid and wall teichoic acid in *Bacillus subtilis*. Identification of genes and regulation. *Journal of Biological Chemistry*, 270, 15598–15606.

Peters, J.M., Colavin, A., Shi, H., Czarny, T.L., Larson, M.H., Wong, S. et al. (2016) A comprehensive, CRISPR-based functional analysis of essential genes in bacteria. *Cell*, 165, 1493–1506.

Pollack, J.H. & Neuhaus, F.C. (1994) Changes in wall teichoic acid during the rod-sphere transition of *Bacillus subtilis* 168. *Journal of Bacteriology*, 176, 7252–7259.

Pooley, H.M. & Karamata, D. (2000) Incorporation of [2-3H]glycerol into cell surface components of *Bacillus subtilis* 168 and thermosensitive mutants affected in wall teichoic acid synthesis: effect of tunicamycin. *Microbiology*, 146, 797–805.

Price, N.P.J. & Tsvetanova, B. (2007) Biosynthesis of the tunicamycins: a review. *The Journal of Antibiotics*, 60, 485–491.

Radeck, J., Fritz, G. & Mascher, T. (2017) The cell envelope stress response of *Bacillus subtilis*: from static signaling devices to dynamic regulatory network. *Current Genetics*, 63, 79–90.

Roberts, A.P. & Mullany, P. (2009) A modular master on the move: the Tn*916* family of mobile genetic elements. *Trends in Microbiology*, 17, 251–258.

Schlag, M., Biswas, R., Krismer, B., Kohler, T., Zoll, S., Yu, W. et al. (2010) Role of staphylococcal wall teichoic acid in targeting the major autolysin Atl. *Molecular Microbiology*, 75, 864–873.

Showsh, S.A. & Andrews, R.E. (1992) Tetracycline enhances Tn*916*-mediated conjugal transfer. *Plasmid*, 28, 213–224.

Skurray, R.A. & Reeves, P. (1973) Characterization of lethal zygosis associated with conjugation in *Escherichia coli* K-12. *Journal of Bacteriology*, 113, 58–70.

Smith, J.L., Goldberg, J.M. & Grossman, A.D. (2014) Complete genome sequences of *Bacillus subtilis* subsp. *subtilis* laboratory strains JH642 (AG174) and AG1839. *Genome Announcements*, 2, e00663-14.

Soucy, S.M., Huang, J. & Gogarten, J.P. (2015) Horizontal gene transfer: building the web of life. *Nature Reviews Genetics*, 16, 472–482.

Swoboda, J.G., Campbell, J., Meredith, T.C. & Walker, S. (2010) Wall teichoic acid function, biosynthesis, and inhibition. *ChemBioChem*, 11, 35–45.

Tiwari, K.B., Gatto, C., Walker, S. & Wilkinson, B.J. (2018) Exposure of *Staphylococcus aureus* to targocil blocks translocation of the major autolysin Atl across the membrane, resulting in a significant decrease in autolysis. *Antimicrobial Agents and Chemotherapy*, 62, e00323-18.

Walter, J., Loach, D.M., Alqumber, M., Rockel, C., Hermann, C., Pfitzenmaier, M. et al. (2007) D-alanyl ester depletion of teichoic acids in *Lactobacillus reuteri* 100-23 results in impaired colonization of the mouse gastrointestinal tract. *Environmental Microbiology*, 9, 1750–1760.

Wecke, J., Madela, K. & Fischer, W. (1997) The absence of D-alanine from lipoteichoic acid and wall teichoic acid alters surface charge, enhances autolysis and increases susceptibility to methicillin in *Bacillus subtilis*. *Microbiology*, 143, 2953–2960.

Weidenmaier, C. & Peschel, A. (2008) Teichoic acids and related cell-wall glycopolymers in Gram-positive physiology and host interactions. *Nature Reviews Microbiology*, 6, 276–287.

Wiedenbeck, J. & Cohan, F.M. (2011) Origins of bacterial diversity through horizontal genetic transfer and adaptation to new ecological niches. *FEMS Microbiology Reviews*, 35, 957–976.

Wolf, D., Domínguez-Cuevas, P., Daniel, R.A. & Mascher, T. (2012) Cell envelope stress response in cell wall-deficient l-forms of *Bacillus subtilis*. *Antimicrobial Agents and Chemotherapy*, 56, 5907–5915.

Wozniak, R.A.F. & Waldor, M.K. (2010) Integrative and conjugative elements: mosaic mobile genetic elements enabling dynamic lateral gene flow. *Nature Reviews Microbiology*, 8, 552–563.

Wyrick, P.B. & Rogers, H.J. (1973) Isolation and characterization of cell wall-defective variants of *Bacillus subtilis* and *Bacillus licheniformis*. *Journal of Bacteriology*, 116, 456–465.

Xu, Q., Chiu, H.-J., Farr, C.L., Jaroszewski, L., Knuth, M.W., Miller, M.D. et al. (2014) Structures of a bifunctional cell wall hydrolase CwlT containing a novel bacterial lysozyme and an NlpC/P60 dl-endopeptidase. *Journal of Molecular Biology*, 426, 169–184.

Yamamoto, H., Miyake, Y., Hisaoka, M., Kurosawa, S. & Sekiguchi, J. (2008) The major and minor wall teichoic acids prevent the sidewall localization of vegetative dl-endopeptidase LytF in *Bacillus subtilis*. *Molecular Microbiology*, 70, 297–310.

Yasbin, R.E., Maino, V.C. & Young, F.E. (1976) Bacteriophage resistance in *Bacillus subtilis* 168, W23, and interstrain transformants. *Journal of Bacteriology*, 125, 1120–1126.

Young, F.E. (1967) Requirement of glucosylated teichoic acid for adsorption of phage in *Bacillus subtilis* 168. *Proceedings of the National Academy of Sciences of the United States of America*, 58, 2377–2384.

Youngman, P., Poth, H., Green, K., York, K., Olmeda, G., and Wager-Smith, K. (1989) Methods for genetic manipulation, cloning, and functional analysis of sporulation genes in *Bacillus subtilis*. In: Smith, I., Slepecky, R. & Setlow, P. (Eds). *Regulation of procaryotic development*. Washington, DC: American Society for Microbiology Press, pp. 65–87.

SUPPORTING INFORMATION

Additional supporting information may be found in the online version of the article at the publisher's website.